4.7 Force Generation by Dynamic Microtubule Polymers

EL Grishchuk, University of Pennsylvania Perelman School of Medicine, Philadelphia, PA, USA
JR McIntosh, University of Colorado at Boulder, Boulder, CO, USA
MI Molodtsov, University of Vienna, Vienna, Austria
FI Ataullakhanov, Center for Theoretical Problems of Physicochemical Pharmacology, Russian Academy of Sciences, Moscow, Russia; National Research Center for Hematology, Moscow, Russia; Moscow State University, Moscow, Russia

Abbreviations

GDP	guanosine diphosphate
GTP	guanosine triphosphate
MAP	MT-associated protein
MT	Microtubule
PF	protofilament

Glossary

Anaphase A stage of mitosis during which the duplicated chromosomes are segregated to different parts of the cell so they can serve as a complete genome for the next cell cycle. Anaphase is commonly thought of in two parts, A and B. During anaphase A, the chromosomes approach the ends of the mitotic spindle; during anaphase B, the spindle elongates, so the distance between the chromosome sets at the completion of anaphase is greater.

Biased diffusion A special case of the general physical phenomenon of diffusion in which the boundary conditions influence the outcome of the many random walks which comprise a true diffusive process. A simple example is diffusion in one dimension with an impermeable boundary; this constrains the otherwise random walks, leading to a nonrandom distribution of particle positions relative to the boundary. A more complicated case, that is directly relevant to biology, is the case in which the boundary moves. Now particle motions

driven by thermal fluctuations are biased to produce net particle movement in the same direction as motion of the boundary.

Catastrophe   A change in the state of a microtubule such that the polymer goes from a condition of continuous growth to one in which the polymer shortens. Catastrophes are thought to result from the loss of guanosine triphosphate-associated tubulin from the polymer's end. The opposite of a catastrophe is a 'rescue'.

Centromere   A chromosomal locus which directs the segregation of that chromosome by serving as a platform for the assembly of a kinetochore.

Coupler   A macromolecular device which attaches a microtubule or other protein polymer to a load which can then be moved by polymer dynamics.

Forced walk   A proposed mechanism by which the bending tubulin protofilaments, that form at the end of a shortening microtubule, pull on an object which is attached to the polymer wall by an appropriate coupler. Thrust from tubulin bending is thought to push the coupler along the microtubule axis in the direction of microtubule shortening, thereby moving its associated cargo. This mechanism is an alternative to the biased-diffusion mechanism of coupler motion with the end of a shortening microtubule, because the forced walk is driven by chemical energy and it can move even nondiffusing couplers.

Kinetochore   A protein complex which forms on eukaryotic chromosomes at their centromeres. It couples a piece of double-stranded DNA to one or more microtubules of the mitotic spindle.

Metaphase   The stage of mitosis at which all the chromosomes have become attached to the mitotic spindle and are situated near its mid plane. The onset of metaphase is not sharply defined because chromosomes move continuously on and off this mid plane while the cell is in metaphase. The end of metaphase occurs at the onset of anaphase, when the duplicate chromosomes separate and begin to move away from each other.

Microtubule   A cytoplasmic polymer, ubiquitous among eukaryotic cells, which assembles from dimers of the proteins α- and β-tubulin. Microtubules are unbranched and comparatively rigid hollow tubes, ~ 25 nm in diameter and of lengths which can range from a few tens of nanometers to many micrometers. They are used by cells as frameworks on which to organize many cytoplasmic proteins which perform a diversity of motile and morphogenetic functions.

Mitosis   The process by which eukaryotic cells segregate their already duplicated chromosomes in preparation for cell division. The name derives from the Greek word for 'thread', because during the early stages of mitosis, chromosomes become visible in a light microscope as slender threads within the nucleus.

Mitotic spindle   The cellular machine which organizes and segregates a cell's duplicated chromosome during mitosis. In overview, the spindle is a twofold symmetric array of microtubules, some of which interact with chromosomes at their kinetochores and some of which interact with one another to form a mechanical connection between the two spindle ends. The name derives from the resemblance between this structure in some cells and an old-fashioned device for spinning wool into yarn.

Processivity   A property of biological motions along a polymer when they continue for many consecutive steps or achieve motion for a comparatively long distance.

Protofilament   A strand of α- and β-tubulin dimers connected end-to-end. Most microtubules in cytoplasm are made from 13 protofilaments which run parallel to the microtubule axis. These protofilaments are slightly out of register, so their tubulin monomers form a 3-start left-handed helix. Not all protofilaments end at the same position along the microtubule axis, so microtubule ends are often uneven. When a microtubule end is shortening, the protofilaments bend away from the microtubule axis before losing their subunits. *In vivo*, the protofilaments on even elongating microtubules are somewhat flared.

Rescue   Change in the state of a microtubule such that the polymer goes from a condition of shortening to one of net growth. Rescues are the opposite of 'catastrophes'. They are thought to result from the addition of guanosine triphosphate-tubulin to a previously shortening plus end.

Tubulin   A soluble protein which is ubiquitous among eukaryotic cells. There is a family of tubulins, but the most common members are dimers of α- and β-tubulin. γ-tubulin forms a ring-shaped complex with several nontubulin proteins; this 'γ-tubulin ring complex' (γ-TuRC) is the principal initiator of microtubule polymerization in cells. Other tubulin isoforms in eukaryotes are found only in association with centrioles. Recently, several isoforms of tubulin have been found in bacteria and archaea; one such tubulin, FtsZ, is a principal player in bacterial cytokinesis. Both α- and β-tubulin bind guanosine triphosphate (GTP), and this association is necessary for tubulin to polymerize. During the polymerization process, the GTP on β-tubulin becomes hydrolyzed, so the bulk of a microtubule is made from tubulin in which α-tubulin still binds GTP, but β-tubulin has guanosine diphosphate, a form of the dimer which can no longer polymerize.

4.7.1   Microtubules Are Ubiquitous Cytoskeletal Polymers, Essential for Cell Health and Viability

Microtubules (MTs) are heteropolymers of α- and β-tubulin; they are a significant part of the cytoskeleton in all eukarya. They usually assemble and function in a context of numerous MT-associated proteins (MAPs). Some MAPs, like the components of the γ-tubulin ring complex, control the initiation of MT growth *in vivo*; others are motors, such as kinesin and dynein (*see* Chapter 4.17 through Chapter 4.20); a second kind of MAP affects MT stability and rigidity; a fourth couples MTs to one another or to other structures in cytoplasm; and a fifth binds preferentially to the growing MT

end and helps to regulate MT dynamics. An additional set of MAPs, a focus of this chapter, facilitates the coupling of dynamic MT ends to the transport of intracellular cargos.

MTs are important because they contribute to many essential cellular functions. They are the principal fibrous component of the mitotic spindle and are essential for normal chromosome segregation. Their dynamics, not simply their presence, is required for both mitosis and the proper organization of endomembranes. A stable group of MTs forms the backbone of an 'axoneme', the structural element and engine for either a cilium or a flagellum. MTs are also the principal framework for motor enzymes which move membranous vesicles through cytoplasm, including traffic to and from the Golgi apparatus and cell surface during endo- and exocytosis. In nerve cells, MTs accomplish long-range vesicle movements (e.g., transport of vesicles from the cell body to synaptic termini and back). MTs can also serve as tracks to move messenger RNAs to cytoplasmic locations where they will be translated, and viruses from their sites of cell entry to the cell nucleus.

Beyond these specific motile functions, MTs contribute to the establishment and maintenance of cell shape and polarity. Their growing ends can deform the cell membrane, particularly in protozoans, and their organized growth can help cells become anisometric. During these activities they interact with other polymers of the cytoskeleton. For examples, the MT-dependent motor enzyme kinesin can move intermediate filaments to spread them throughout the cell, and some not-yet-well-understood MAPs interact with actin, allowing MTs to influence the organization of microfilaments and vice versa.

Given all these roles, it is no surprise that MTs are essential for the health and function of all eukaryotes. Some MT-dependent cellular processes utilize these polymers as stable, polar tracks (e.g., during the intracellular transport of vesicles by adenosine triphosphate [ATP]-dependent mechanochemical enzymes). Others require dynamic and stochastic features of tubulin polymerization. This chapter focuses on one specific class of MT-dependent processes – those which rely on the ability of dynamic MT tips to exert forces.

4.7.2   Growing MTs Can Push

MTs in cells are in a dynamic equilibrium with soluble α-β tubulin dimers. When conditions favor polymerization, it is no surprise that MTs can push on objects which stand in the way of their growth. This property does not rely on a specific feature of MTs; for example, polymerizing actin can also push,[1,2] and the polymerization of actinlike proteins in bacteria provides force for the segregation of many examples of prokaryotic DNA.[3] Growing biological polymers exhibit such behavior because the characteristic size of their protein subunits is on the nanometer scale, and assembly takes place in an environment in which the average thermal motions of macromolecules exceed their size. The following sections review the best-studied examples of MT pushing *in vivo* and *in vitro*, and describe the underlying theoretical models, that are quite advanced and show a good correlation with experimental data *in vitro*.

4.7.2.1   Experimental Evidence

The ability of MT growth to deform cellular structures was first appreciated in studies of the protozoan *Echinospherium*, a heliozoan with MT-containing arms which radiate from a spherical cell body by hundreds of micrometers. Removal of these MTs by treatments with cold, hydrostatic pressure, or tubulin-binding drugs led to withdrawal of the cellular arms. Upon reversal of the perturbation, MTs regrew and the arms reappeared.[4] In more recent experiments, MT growth has been shown to define the position of the cell nucleus in fission yeasts,[5] drive the motility and distribution of mitochondria in fission yeast,[6] and alter the structure of endoplasmic reticulum in newt lung epithelial cells.[7] These observations show that tubulin polymerization can modify both the position and shape of cellular organelles.

The simple interpretation of these experiments in cells can be challenged because the complexity of cytoplasm admits the possibility that some other factor, like a motor or another filament system with a distribution which depends on MTs, is doing the actual work of deforming the cell or its contents. This criticism is not pertinent, however, when purified components are used. The most direct demonstration of MT polymerization-dependent pushing is the ability of pure tubulin dimers in liposomes to polymerize and deform the shape of their lipid envelope (Figure 1(a)).[8,9] Also, an MT end can be observed directly as it grows against a rigid wall, leading either to MT buckling or to a push on the bead-attached MT initiator (Section 4.7.2.3). When tubulin polymerizes in a confined, microfabricated chamber from an object which nucleates numerous MTs (e.g., an isolated centrosome), pushing forces from the resulting aster can position the nucleator in the geometric center of the chamber, providing an attractive *in vitro* model for the centering of nuclei in fission yeast cells.[10,11] Larger cells, in which MTs grow longer, almost certainly use additional means to find their centers (e.g., with the help of dynein-dependent pulling).[12] Even in fission yeast, other processes – such as interactions between MT tips, kinesins, and cortex-associated modulators – are also at play.[13,14] Nonetheless, numerous studies *in vivo* and *in vitro* clearly establish the ability of growing MTs to push, suggesting that these processes are important in cells.

4.7.2.2   Theoretical Model of Pushing by a Single-Strand Polymer

A simple model of the pushing forces generated by polymerization is provided by considering the tip of a single-strand filament which grows against a fluctuating particle. Thermal motion in this system is fundamental to its operation, so this and analogous molecular mechanisms have been termed 'Brownian ratchets'.[15] The particle's motion ahead of a growing filament provides an opportunity for a monomer to add on to the polymer's tip, thereby extending its length by δ (Figure 1(b)). Such an event is called 'rectification' because it prevents the particle from moving back, thereby working as a ratchet.
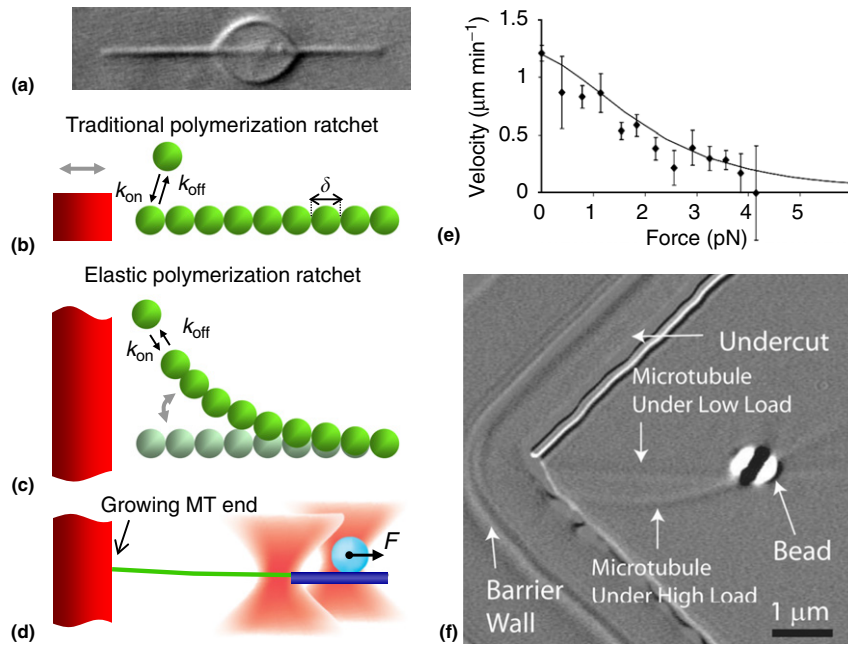
Figure 1   Forces exerted by growing microtubules (MTs). (a) A phospholipid vesicle is deformed by growing MTs. Differential interference contrast image adapted with permission from Fygenson, D. K.; Marko, J. F.; Libchaber, A. Mechanics of microtubule-based membrane extension. *Phys. Rev. Lett.* **1997,** *79*, 4497–4500. Copyright by American Physical Society. (b) The simplest single filament polymerization ratchet assumes that the filament (green) is infinitely stiff and the Brownian motion of the load alone (gray double-headed arrow) creates a gap sufficient for monomers to intercalate between the polymer tip and the load (red). (c) In the 'elastic Brownian ratchet', bending motions of the filament (gray double-headed arrow) open a gap for subunit incorporation between the polymer tip and the motionless load. (d) An experimental system to study force generation by a single polymerizing MT. MT (green) growing from the bead-associated axoneme (dark blue) pushes against a barrier and forces the bead to move in the opposite direction. Two red cones represent a 'keyhole' laser trap. (e) Force-velocity relationship for growing MTs. Circles correspond to experimental data.[21] The solid line is predicted by a ratchet model for 13 independently growing parallel filaments. Reproduced from Dogterom, M.; Janson, M. E.; Faivre-Moskalenko, C.; van der Horst, A.; Kerssemakers, J. W. J.; Tanase, C.; Mulder. B. M. Force generation by polymerizing microtubules. *Appl. Phys. A* **2002,** *75*, 331–336, with permission from Copyright by Springer. (f) Differential interference contrast micrograph of an experiment showing an MT, its attached bead, and a barrier. Two images were superimposed to show the MT before it was loaded and after, at which time it buckled. Reproduced from Schek, H. T., III; Gardner, M. K.; Cheng, J.; Odde, D. J.; Hunt, A. J. Microtubule assembly dynamics at the nanoscale. *Curr. Biol.* **2007,** *17*, 1445–1455.

In the presence of a constant load F, the velocity of polymerization v is given by

$$v(F) = \delta(k_{on}e^{-F\delta/k_BT} - k_{off})$$ [1]

where δ is monomer size, and k_{on} and k_{off} are rate constants of polymerization and depolymerization, respectively. With this approach, the depolymerization rate is generally assumed to be unaffected by the presence of the force, although this assumption is a subject for debate.[16]

Equation [1], derived by Peskin et al.[15] has a simple interpretation: Under load, the polymerization rate is modified by the Boltzmann factor $\exp(-F\delta/k_BT)$ (i.e., the probability of opening a gap δ under the force F). From this expression, it is easy to derive the stall force, that is defined as the force needed to bring the growth velocity to zero:

$$F_{stall} = \frac{k_BT}{\delta}\ln\frac{k_{on}}{k_{off}}$$ [2]

This consideration treats the filament as a stiff rod, so thermal fluctuations affect only the motion of the particle. However, when the converse is true (e.g., the particle is replaced with a solid wall and the filament is elastic), the behavior of the system is not changed. Even if the monomer's addition to the

end of the filament is hindered because the distance to the motionless wall is smaller than the size of the monomer, Brownian fluctuation bends the filament, whereupon a monomer may be able to attach to its end (**Figure 1(c)**). The statistical motion of a filament tip is subject to a harmonic restoring force, resulting in pushing against the load. The corresponding mechanism is called an 'elastic Brownian ratchet'. It is applicable to any polymer which meets the following requirements:[17] (1) thermal bending fluctuations are fast in comparison with the assembly process; (2) the filament bends much more easily than it compresses, so the major mode of thermal motion is bending; and (3) for small deformations, the elastic energy of bending is less than thermal energy. With these assumptions, the assembly rate for a filament under load is altered by the same Boltzmann factor, as in eqn [1].

These postulates are met by tubulin polymers, albeit with some restriction on their length. The first assumption is easily satisfied because the polymerization and depolymerization rate constants for tubulin dynamics are relatively low. However, MTs are quite rigid, with a flexural rigidity of $\sim 2 \times 10^{-23}$ N m²,[8] so the above assumptions (2) and (3) are true only for relatively long polymers. One can estimate the minimal length of a tubulin polymer which would behave as

an 'elastic Brownian ratchet' by taking into account that MTs assemble by the addition of 8-nm-long tubulin dimers. However, each MT normally consists of 13 strands, called 'protofilaments', in which tubulins form a 3-start helix, so the minimal advance of the leading tip is roughly $12/13 = 0.9$ nm. Calculations show that a gap of this size between the MT tip and a rigid barrier is formed by 1 k_BT energy if MT length is about 2 μm, although in some models the necessary length has been said to be significantly greater.[19] Thus, MTs shorter than 2 μm do not satisfy assumption (3). Bending of such short polymers requires relatively significant thermal energy, so the incorporation of a subunit must await a sufficiently large thermal fluctuation, thereby limiting the effectiveness of the elastic pushing by such polymers. Furthermore, these stall periods may lead to a catastrophe – a sudden switch from MT growth to shortening.[20] Very long polymers also do not push well, but for a different reason; MTs longer than 10 μm buckle under a force more than 5 pN.[11]

4.7.2.3 Experimental Analysis of Pushing by Growing MTs

Dogterom et al.[10,21] have developed an *in vitro* system to study MT pushing in microfabricated wells. Force generated by a single growing MT has been measured by using short pieces of stabilized MTs attached to glass substrate via a biotin-streptavidin linkage. Purified soluble tubulin in the presence of guanosine triphosphate (GTP) polymerizes from these seeds. The elongating polymer can then be observed to encounter a barrier made from lines of vapor-deposited SiO. Some MTs start to buckle, pivoting around a fixed contact with the barrier.[10] In a more advanced version of this experimental approach, an axoneme (the MT-based framework of a cilium or flagellum) was attached to a micron-sized bead (**Figure 1(d)**). A 'keyhole' optical trap was used (i.e., a combination of a single point trap and a line trap). To create a keyhole trap, a laser beam is moved periodically along a linear segment using an acousto-optical deflector. The most visited position serves as a trap for the bead, whereas trapping along the linearly distributed positions helps to orient the axoneme and direct MT growth toward a barrier.[22,23] When the growing MT end pushes against the barrier, it forces the axoneme-attached bead to move in the opposite direction. Therefore, in a calibrated trap, the bead's displacement can be used to measure the force generated by MT growth. This and previous mentioned approaches have produced consistent results and have provided experimental determination of the effect of compressing force on MT growth (**Figure 1(e)**[21]). With increasing load, the rate of MT polymerization decreases, and growth stalls at about 5 pN, a result similar to predictions by the 'elastic Brownian ratchet' models, that combine 13 single-strand filaments (Section 4.7.2.5).[19,24] Furthermore, these studies have established interesting relationships between compressive forces and MT dynamic instability, leading to the discovery of compression-induced catastrophes.[20]

4.7.2.4 Nanoscale Analysis of the Assembly at the MT Tip

The introduction of laser trapping into the study of MT growth *in vitro* has significantly improved the accuracy of measurement and opened an avenue by which to examine molecular events which take place at growing MT ends. Two recent studies have analyzed fine details of tubulin addition to MTs which were nucleated from bead-associated axonemes.[22,25] In one, a keyhole optical trap was used to control both the position of the bead and the direction of MT growth, as described earlier. In the second study, MTs grew from bead-associated seeds toward a corner formed by two barrier walls, so the pushing MT tip could not move (**Figure 1(f)**). Following the growing tip's contact with the barriers, motions of the MT-attached beads were tracked with up to 3.5-nm precision. The exact interpretations from these two similar studies are, however, quite different, most likely because of different trapping regimes, different resolutions of measurement, and the ways in which the data were collected and processed. From one such study, tubulin assembly at the MT tip was suggested to proceed in ∼25-nm steps, that is significantly larger than expected if a single tubulin dimer (8 nm in length) is the attachment intermediate.[22] The second study suggests, however, that MT growth occurs with no detectable steps, but via alternations of highly variable growth and shortening excursions which range up to 40 nm in size.[25] Together, these results point to a polymerization scenario which is more complex than is implied by the current models of MT assembly, most likely because they do not consider the elastic properties of the variable protofilament protrusions. Further application of these sensitive techniques will undoubtedly help to reveal a detailed picture of tubulin dynamics at the MT tip, and promote development of a comprehensive mathematical model of MT assembly.

4.7.2.5 Toward a Unified Model of MT Growth

The complexities of novel experimental methodologies have highlighted the need for building a realistic MT model which would combine a detailed molecular description with the polymer's mechanics and important aspects of MT physiology. Theoretical modeling has so far moved in two directions. In the first, a 13-protofilament MT growing against the rigid barrier has been modeled by building on the Brownian ratchet models for single filaments. When 13 protofilament tips polymerize against a wall, their collective dynamics are based on the explicit equations for the tip's continuous spatial density.[19] The resulting pushing force, however, does not scale proportionally with protofilament number, N, because of the complex geometry of the MT tip and lateral interactions between protofilaments. The following expression, derived by Mogilner and Oster,[19] describes MT growth at large load forces rather well:

$$v(F) = \delta(k_{on}N\left(\frac{k_BT}{F\delta}\right)^2 - k_{off}) \qquad [3]$$

Here, δ is no longer the monomer's length, because of the stochasticity of subunit addition to multiple protofilaments.

In a slightly different approach, the push generated by a complex 13-filament tip was studied by introducing (1) the parameter q to represent the load distribution factor, that determines the degree to which the load affects the on vs. off rates for subunit association, and (2) parameters d_0 and d_1,

that describe the tip's geometry.[16] In this model, the force-velocity relationship is given by

$$v(F) = d_0(k_{on}e^{-qFd_1/k_BT} - k_{off}e^{(1-q)Fd_1/k_BT})$$ [4]

where Fd_1 represents the most probable work needed to add a single tubulin dimer against the load F. The effect of the Boltzmann factor on k_{off} is, however, small, so this description is similar to eqn [3].

In summary, these phenomenological models provide a good fit to the experimental force-velocity curve, but their usefulness in describing more complex experimental data is limited, and they provide little insight about the molecular details of MT growth. The difficulty lies in the complexity of tip geometry and a lack of detailed information about the interactions between adjacent protofilaments. These obstacles lead to a large number of model parameters or assumptions, hindering further developments in this direction. A radically different description has been introduced by molecular-mechanical modeling, during which individual tubulins are described as separate mechanical elements.[26,27] They interact with each other via potential functions which are dependent
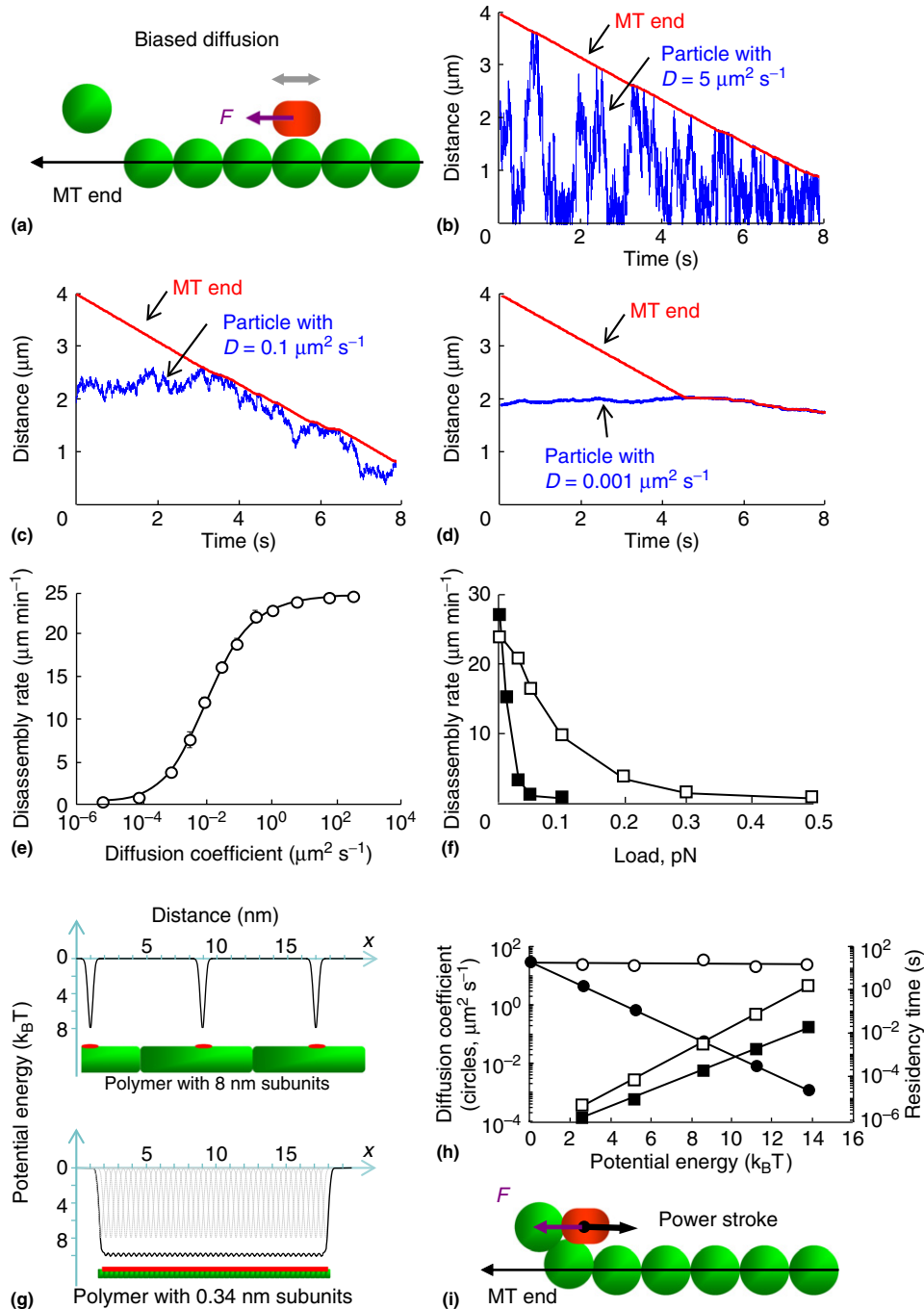
on the state of bound guanine nucleotide. Such an approach has proved to be particularly valuable in studies of forces developed by depolymerizing MTs, so the corresponding model of the shortening MT is described in Section 4.7.4.1. A three-dimensional 'mechanochemical model' by Odde and colleagues[28] explicitly combines tubulin assembly kinetics with the mechanical forces acting between tubulins in the MT lattice. Future incorporation of the elasticity of individual protofilaments and their variable protrusions into this model will help to bring theoretical modeling up to a level of refinement appropriate for interpretation of the nanoscale studies of MT assembly.

4.7.3 Shortening MTs Can Pull on a Load in at Least Two Ways

In recent years, there has been a surge of interest in depolymerization as a possible source of energy for mechanical work in cells. Force production by depolymerizing MTs is especially important to study because MT disassembly is known to play an essential role in chromosome motions during cell division. *In vitro*, MT depolymerization can move both chromosomes and microspheres in an ATP-independent way.[29,30] A genetic analysis of factors essential for chromosome-to-pole motion in yeasts has shown that minus-end-directed, MT-dependent motor enzymes are not required for poleward chromosome movement, so MT disassembly is likely to be the primary motor for these motions.[31,32] Because loss of a chromosome can lead to severe pathologies, there has been a significant effort to understand how MT depolymerization can transport a cargo with high fidelity. The following sections highlight two established mechanisms by which energy stored in MTs can be converted into useful work during depolymerization – a biased-diffusion mechanism and a power stroke-dependent mechanism, which is based on the unusual mechanochemical pathway of MT disassembly.

4.7.3.1 Particles Can Move with Shortening MT Ends by a Biased-Diffusion Mechanism

The ability of MTs by themselves (i.e., in the absence of motor enzymes) to generate pulling forces is less intuitive than the development of pushing forces. Moreover, only one other nonextensible polymer has been reported to do such a job, in cells or otherwise,[33] but a credible mechanism for motion with this shortening polymer has not yet been developed. MTs shorten by losing subunits from their ends, so it is difficult to imagine that a cargo can move by hanging on to the disassembling polymer tip. Nonetheless, a polymer which is reducing the free energy of the system by shortening can, in theory, do work by biasing the diffusion of a molecule associated with its wall. There are different diffusion-based models in which the necessary bias is created by Brownian ratchets.[34] For example, in the 'burnt bridge' model, a particle which moves only along the polymer's surface destroys its tracks after crossing them in a one direction, so the particle's backward motion is prevented.[35] These models do not take a direct advantage of a mechanochemical pathway of MT disassembly, so they are applicable to any shortening polymer, not just MT.

To highlight the specific features of such diffusion-based mechanism, the authors consider a simplified version of a motile system consisting of a single-strand polymer with N subunits (e.g., a single protofilament in an MT wall) and a particle (an MT-binding protein) which can bind to tubulin subunits (**Figure 2(a)**). To simplify their consideration even further, they assume that the particle can move along the protofilament, but it cannot detach from its surface completely, even as it 'hops' from one binding site to the next. In an MT lattice, the binding sites are located 4 nm or 8 nm apart, depending on whether the protein binds to each tubulin monomer or to a dimer. Obviously, the simplifying assumption that the particle always remains associated with the polymer is not true for traditional, site-specific protein-protein interactions, that occur through an alternation between bound and unbound states (Section 4.7.3.4). Although the nature of interactions between the MT polymer and diffusing MAPs is not yet known, the duration of their diffusive motions is limited. For example, the heterodecameric Dam1 protein remains bound to MT for only 2 s,[36] and the Ndc80 kinetochore protein detaches in less than a second,[37] although some proteins can maintain their diffusive attachment for much longer (40 s for single-headed myosin Va).[38]

Figure 2 Mechanisms of a microtubule (MT) depolymerization-dependent motion. (a) In a biased-diffusion mechanism, thermal fluctuations drive a particle's random walk (gray double-headed arrow), whereas the shortening polymer end biases this motion to produce directionality. The load F causes the particle to shift toward the polymer's end, where its continued attachment requires some retention mechanism, or the particle will be lost. (b)–(d) Calculated positions (in blue) of particles moving via diffusion which is biased by the shortening polymer end (red line). Calculations were carried out with eqn [5]. The depolymerization rate for a particle-free polymer is 25 μm min^{-1}, the polymer's end serves as a boundary, and other parameters are as noted in the text. (e) Calculated rate of polymer disassembly as a function of the diffusion coefficient for the associated particle. Calculations were carried out for a 100-μm-long single-strand polymer, that disassembled at 25 μm min^{-1} in 8-nm steps. To avoid the particle's loss at the polymer's end, the terminal subunit was allowed to detach only if it was particle free for ≥ 0.02 s, that is the average time of tubulin dimer dissociation in an MT which shortens at the noted rate. Error bars are standard error of the means for at least five simulations for each data point. (f) The rate with which the particle tracks the shortening polymer end as a function of load F. Diffusion coefficient $D = 0.08$ and 5 μm^2 s^{-1} for open and closed symbols, respectively. (g) Potential energy landscape for particle-polymer interactions, one binding site (red) per subunit (scale is approximate). When the wells are close together, as in a polymer with 0.34-nm subunits, they merge to form a valley (thick black curve), such that the energy barriers for particle diffusion become smaller than in the original wells (thin black curves). When distance between the adjacent potential wells is significantly larger than the depth of the energy well, the valley is not formed and the barriers for protein diffusion and for the unbinding from the polymer are virtually identical. (h) Calculated diffusion coefficients (right y axis, circles) and residency time (left y axis, squares) for a particle diffusing on the linear polymer with 8-nm subunits (closed symbols) or 0.34-nm subunits (open symbols) as a function of parameter A (eqn [6]). Residency time was calculated as the mean time that a particle spends in a bound state. For 0.34-nm subunits, the same potential (eqn [6]) was used, but A was chosen to be equal to the depth of the merged well. (i) In a forced-walk mechanism, the particle moves at the polymer's end as a result of a power stroke exerted by a terminal subunit prior its dissociation (black arrow).

The change in position of the theoretical particle over time, as it diffuses on the polymer's surface, can be obtained using a Brownian dynamic algorithm.[39] In general terms, if the motion takes place in a viscous medium and the particle is under a load, F,

$$x_{i+1} = x_i + \frac{\tau}{\gamma} F_i(x) + \sqrt{2D\tau} p_i \qquad [5]$$

where x_i is the particle's position at any time t, x_{i+1} is the particle's position at time $t + \tau$, γ is frictional coefficient (138 pN s m^{-1} in water), and p_i is a random number from a normal distribution with zero mean and $\sigma = 1$. The diffusion coefficient, D, for a protein with a molecular weight of 100 kDa in water is $\sim 30\ \mu m^2\ s^{-1}$, although diffusion for such particles in cytoplasm is about 10 times slower.[40]

Let us first consider the case when the particle does not carry any load ($F = 0$). It easy to see that the particle's motion will become biased if the polymer starts to shorten. If the polymer-bound protein diffuses relatively fast, it travels back and forth many times during the time of polymer shortening (Figure 2(b)). Because the authors have assumed that the protein does not dissociate from the polymer, every time the particle encounters the polymer's end, it does not detach, but simply changes the direction of its motion, as if encountering a reflecting barrier. The mean position of the fast-diffusing protein particle is in the middle of the polymer, moving gradually in the direction of shortening. In fact, on a growing polymer such a particle would show biased motion in the opposite direction, as long as the polymer is not so long that the particle rarely encounters its boundaries. A particle that diffuses more slowly (e.g., with a diffusion coefficient similar to Dam1 heterodecamer [$D = 0.08\ \mu m^2\ s^{-1}$][36] and Ndc80 protein [$0.15\ \mu m^2\ s^{-1}$][37]) does not move far before the shortening polymer end catches up. Thereafter, such a particle also shows directed net motion, but it stays closer to the shortening tip (Figure 2(c)). In both examples, the rate of net particle motion is determined primarily by the rate of the polymer's disassembly. MTs disassemble *in vitro* at 20 to 30 $\mu m\ min^{-1}$, so proteins which maintain their attachment for only 1 to 2 s can be transported by the shortening MT for about 0.6 μm, a significant distance on the scale of a cell. However, *in vivo*, the MTs often shorten more slowly. For example, MTs which attach to kinetochores of mammalian mitotic chromosomes disassemble at 1 to 2 $\mu m\ min^{-1}$, so they can move a diffusing protein, such as the Dam1 heterodecamer, for only about 40 nm, the length of five tubulin dimers, before such a particle detaches from the MT surface.

4.7.3.2 Biased Diffusion of a Slow Particle Can be Processive Only If It Inhibits Dissociation of Polymer Subunits

A different scenario is expected for a particle which diffuses even slower than those in Figure 2(b) and (c). If the particle's mean first passage time to move from one site to the next is comparable with the average dissociation time for a terminal polymer subunit, after the shortening end catches up with the particle, the subsequent behavior of this system depends on the exact mode of interaction between the particle and the

polymer's end. If depolymerization can proceed regardless of the particle's terminal position, then the particle is lost quickly, while still attached to the dissociated subunit; end tracking by such a particle is not possible. However, if we assume that the end subunit cannot dissociate until the particle advances to the next binding site, this system will exhibit directional motility. In this case, however, the particle's diffusion is rate limiting (Figure 2(d)). Note that a slight inhibition of MT depolymerization can be seen in this model, even with faster diffusing particles, whenever they happen to spend more time at the shortening MT end (Figure 2(b) and (c)). Figure 2(e) shows, however, that the slower the particle's diffusion, the stronger its impact on the rate of polymer disassembly. From this graph, one can estimate a minimal value of the diffusion coefficient for which the particle produces little inhibition on the polymer's disassembly – approximately $10^{-1}\ \mu m^2\ s^{-1}$ and $10^{-4}\ \mu m^2\ s^{-1}$ for the disassembly rates which correspond to MT depolymerization *in vitro* and for chromosome motion *in vivo*, respectively. Many known MT-associated proteins diffuse faster than this limit,[41] including the Dam1 heterodecamer. However, the oligomeric assemblies of this protein, that contain several Dam1 heterodecameric subunits, diffuse significantly slower,[42] so they should slow MT depolymerization, as is indeed observed.[43] Although the exact value of the diffusion coefficient of the 16-subunit Dam1 complex, as found in the MT-encircling Dam1 ring,[44] is not known, the authors have previously estimated that it is $\leq 10^{-5}\ \mu m^2\ s^{-1}$.[44] If such a large complex moved with the shortening MT end via the biased-diffusion mechanism, it should reduce the rate of MT disassembly to 0.1 $\mu m\ min^{-1}$. The fact that the Dam1 oligomeric complexes of this size track the shortening MT ends *in vitro* at 7 to 10 $\mu m\ min^{-1}$ strongly suggests that their motion is driven by a different, energy-consuming mechanism (see Section 4.7.5).[43]

4.7.3.3 A Biased-Diffusion Mechanism Cannot Carry a Large Load

The authors now consider briefly the biased diffusion of a particle in a force field. With increasing load F, the particle's average position shifts toward the polymer's end and the particle spends more time bound to the last subunit (eqn [5]). If we continue to assume that the terminal subunit with a bound particle cannot dissociate from the polymer, this rule will ensure that the particle is not lost and always remains bound to the polymer. However, the rate of polymer depolymerization will necessarily slow down. Even for the fast-diffusing proteins ($D = 5\ \mu m^2\ s^{-1}$), a load of 0.01 pN slows the depolymerization-dependent motion twofold, whereas the load of 0.1 pN stops polymer disassembly all together (Figure 2(f)). This inhibitory effect is slightly less strong for slower diffusing particles. For example, a particle with the same diffusion coefficient as the Dam1 heterodecamer should slow MT depolymerization to 1 $\mu m\ min^{-1}$ if the Dam1 particle carries a 0.3-pN load *in vitro*, whereas the 0.5-pN load should block the motion completely (Figure 2(f)). In the absence of the above assumption (i.e., if the rate of polymer depolymerization remains constant and is unaffected by the particle's position), the increasing load increases the probability that

the particle will detach together with the terminal subunit. For example, a 0.5-pN load applied to a particle which diffuses on an MT shortening at 2 μm min⁻¹ causes the particle to shift to the terminal subunit and to detach in about 0.2 s. Thus, in a biased-diffusion mechanism, a comparatively small load (<1 pN) either completely blocks the polymer's disassembly or leads to a rapid loss of a tip-associated cargo for a wide range of diffusion constants.

It is difficult to describe accurately a load dependency for polymer end tracking in a more biologically relevant case (e.g., when a polymer with 13 protofilaments serves as a track for the diffusion of several interconnected proteins). Such analysis requires detailed information about the protein-polymer interactions, and about the structure and interactions within the protein ensemble. Several examples of such studies are described in Section 4.7.5. However, one can roughly estimate the maximum force which can be sustained by a set of independently diffusing particles by assuming that the MT depolymerization force scales with the number of protofilaments (see Section 4.7.4 for justifications). Thus, a shortening MT can carry a load of 0.3 pN × 13 ≈ 4 pN at 1 μm min⁻¹ with the help of particles with diffusion coefficients which resemble the Dam1 heterodecamer; the motion stalls at 6 to 7 pN. If the particles form a specific structure (i.e., their diffusive motions are not independent), the stalling force is determined by the design of such a structure. The maximal known force for a diffusing multiparticle device is achieved with Hill's sleeve (see Section 4.7.5), where the stalling force is 9 to 15 pN.[27,45,46] This is fivefold less than what is believed to be the maximum force which the kinetochore-associated MTs can withstand before stalling.[47] In summary, the authors conclude that biased-diffusion mechanisms can drive MT depolymerization-dependent motion of small particles (e.g., individual proteins) and even larger objects, like micron-sized beads. In an aqueous environment, the viscous drag on these objects is so small that they move at modest speeds with essentially no load. The viscous drag on mitotic chromosomes moving through cytoplasm is also very small,[47] so these motions, too, could – in principle – be powered by biased diffusion. However, chromosome motions under larger loads, such as in spermatocytes,[47] cannot be explained by thermal diffusion. This intrinsic property of a diffusion-based pulling mechanism raises doubts about its possible role in chromosome motion, especially in organisms in which moving chromosomes may naturally encounter large opposing forces.

4.7.3.4 Energy Landscape for the MT Surface Is Likely to be Rough

The above consideration of particle-polymer interactions has used the simplifying assumption that the particle can move along the protofilament by hopping from one binding site to the next, but it cannot detach from its surface completely. Here, the authors analyze how the particle's residency time (i.e., the time during which the particle remains bound to the polymer) and particle's diffusion depend on the particle-polymer binding energy.

Interaction between the particle and polymer's subunit can be described by a potential energy function $U(x)$, where x is a linear coordinate along the polymer. For simplicity, the authors use a Gaussian function to represent $U(x)$:

$$U(x) = -A\sum_i \exp\left(-\frac{(x - x_i)^2}{r_o^2}\right) \qquad [6]$$

where A and r_o are the depth and width of the potential energy well, and x_i is the position of the well's center. The sum is for all wells on the polymer. For typical protein-protein interactions, the width of the potential well is 0.2 to 0.5 nm (**Figure 2(g)**).[48,49] Here, the authors assume that $r_o = 0.24$. Furthermore, the authors continue to assume that the particle has only one binding site per monomer, so the energy wells are separated by the distance which equals the monomer's size; the exact location of the energy well on the monomer's surface does not affect this model's conclusions.

The size and nature of the potential energy well for proteins diffusing on MTs is not yet known, but it is often assumed that the wells are so shallow that it would be more appropriate to treat this energy landscape as an 'isoenergetic microtubule domain'.[41] For example, it has been suggested that proteins like Dam1 may bind anywhere on the MT's surface with "no specific footprint"[50] such that they slide on the MT surface without significant friction. Some DNA-binding proteins are known to diffuse along nucleic acid threads,[51] and the MT-dependent diffusion has been suggested to be analogous.[41] To examine this view, the authors analyzed a particle's diffusion along a polymer in which the adjacent binding sites are separated by energy barriers:

$$x_{i+1} = x_i + \frac{\tau}{\gamma}\frac{\partial U}{\partial x_i} + \sqrt{2D\tau}p_i \qquad [7]$$

where $\frac{\partial U}{\partial x_i}$ is the potential energy derivative at time t; see eqn [5] for details.

Diffusion coefficients have been calculated as a function of particle-polymer binding energy for polymers with 8-nm (tubulin dimer) and 0.34-nm (length of nucleotide pair in DNA) subunits. **Figure 2(h)** shows that diffusion on both polymers decreases exponentially with increasing depth of the energy well. When the wells are positioned 8 nm apart (one interaction site per tubulin dimer), this dependency is steep and the diffusion slows down 10-fold per 2.7-k_BT increase. For example, 8-k_BT energy wells on a tubulin polymer should slow the diffusion from 30 μm² s⁻¹ (seen for a free particle in aqueous solution) to 0.1 μm² s⁻¹. The particle's residency time, however, increases exponentially with increasing binding energy.

Diffusion results on polymers with much smaller subunit size are, however, quite different. A 10-fold deceleration of diffusion on a polymer with 0.34-nm subunits would require unrealistically deep energy wells – 65 k_BT. In other words, a particle can diffuse fast on a linear polymer with small subunits even if the binding is very strong. Such unusual behavior results from the subunit being smaller than the width of the potential well, causing the adjacent wells to merge and form a complex energy landscape which has been appropriately called a 'potential valley' with some 'roughness' (**Figure 2(g)**),[52] that for DNA is estimated to be on the order of 1 k_BT.[53,54] In a deep 'valley' (its depth slightly exceeds the

depth of an unmerged well) with such small barriers, diffusion is fast and the residency time is longer than what is seen for the same diffusion coefficient on a polymer for which the wells are distantly separated.

Interestingly, the diffusion coefficient for DNA-binding protein is in the 0.1-1-$\mu m^2\ s^{-1}$ range,[53] one to two orders of magnitude slower than predicted by the authors' calculations. This discrepancy is explained by the rotation which must accompany the diffusion of particles on DNA, but not on linear polymers (eqn [7]). Because DNA forms a helix, DNA-binding proteins must not only move collinearly with the DNA axis, but they also must spin around the helix axis.[53,55] This additional motion implies a friction which slows DNA-dependent diffusion. Nonetheless, the diffusion coefficient is still expected to depend weakly on binding energy, because of the 'potential valley' formed by DNA. In a typical MT polymer (13_3 configuration), all protofilaments run parallel to each other, so no motion around the polymer axis is required. Therefore, tubulin-binding proteins are likely to exhibit a simple, one-dimensional diffusion along these strands. Thus, a theoretical 'upper bound', the limit imposed on diffusion coefficients for spinning DNA-binding proteins,[55] does not apply to MT-dependent diffusion.

This consideration demonstrates the significant differences between the physics of particle diffusion on polymers with different geometries, so the suggested analogy between DNA and tubulin appears to be inappropriate. The energy landscape for the MT surface is likely to be very rough, as suggested, for example, by the calculated potential isocontours for the MT polymer,[56,57] that reveal periodicity at 8- and 4-nm steps, but nothing much smaller. Furthermore, as illustrated earlier, on a polymer surface with distantly separated energy wells, particle diffusion should depend strongly on its binding energy. The existing measurements for the diffusion on MTs are consistent with these expectations. For example, positively charged polyacrylamide nanoparticles have been shown to exhibit one-dimensional Brownian motion along MT polymers.[58] These interactions are clearly different from the typical 'lock-and-key' protein-protein association – an observation that opens the possibility that some MAPs might also diffuse via a binding that is not specific to the MT structural landscape. However, even in this case, the particles with a diffusion coefficient $\sim 0.3\ \mu m^2\ s^{-1}$ were estimated to move in the energy landscape with 2-k_BT wells, which is more 'rough' than for DNA-binding proteins. Nanoparticles with more charge diffused even more slowly, with activation barriers estimated to be as great as 4.2 k_BT.[58] Diffusion of most MT-binding proteins is usually even slower, including the previously mentioned Ndc80 and Dam1 protein complexes. The single-headed kinesin KIF1A diffuses at 0.04 $\mu m^2\ min^{-1}$,[59] that is estimated to correspond to 6.5-k_BT activation barriers.[58] The dimeric kinesin motor Kip3 has 10-fold slower diffusion, that has been shown to occur with 8-nm steps.[60] Thus, this protein appears to bind to the MT surface via a traditional site-specific interaction with the estimated energy barrier of $\sim 13\ k_BT$.[60]

Overall, the measured diffusion coefficients and estimated energy functions for MT-dependent diffusion are consistent with the simple model described by eqns [6] and [7]. It should be noted, however, that the measured residency time for MT-diffusing proteins is significantly longer than those predicted by

this model. According to Figure 2(h), the MT-binding protein with $D = 0.1\ \mu m^2\ s^{-1}$ is expected to remain bound to MT for only 0.2 ms. This prediction is relatively insensitive to the assumption that the energy well is narrow. For example, if r_o is increased approximately sevenfold (1.6 nm), the residency time increases only 2.5-fold. This time is almost 10^4 times shorter than what is measured, for example, for the Ndc80 complex.[37] This discrepancy suggests that the interaction between some MT-binding proteins and tubulin subunits is more complex than what is assumed in this model with one binding site between the protein and polymer subunit. Indeed, the binding interface between Ndc80 and MT is likely to involve two binding sites.[61,62] Furthermore, both α- and β-tubulins have negatively charged C termini, which contribute to the binding of some MAPs. Thus, the molecular details of the interactions between MTs and specific proteins, as well as their corresponding energy potentials, remain to be determined.

4.7.3.5   MTs Are Reservoirs of Chemical Potential Energy

MTs are unusual polymers in permitting not only the very general biased-diffusion mechanism for force generation through depolymerization, but also a mechanism which depends directly on the specific pathway by which tubulin adds to and leaves the MT end. Soluble tubulin binds two molecules of GTP – one at an exchangeable site on β-tubulin and one at a nonexchangeable site on α-tubulin (see Chapter 4.6). As GTP-associated tubulin dimers polymerize, the nucleotide triphosphate bound to β-tubulin is hydrolyzed, so most of the tubulin in an MT is guanosine diphosphate (GDP) associated at this site. However, when GDP occupies the β-tubulin site on soluble tubulin dimers, the protein won't polymerize.[63] MTs are therefore built from tubulin which won't assemble into a lattice – a situation that is thought to account for the fact that MTs can undergo 'catastrophes', in which slow polymerization is suddenly changed into a rapid depolymerization. This behavior has been termed 'dynamic instability'.[64]

Structural studies suggest that a tubulin dimer with GDP bound to its β subunit is bent so it won't fit into an MT wall.[65] Thus, polymerized GDP-tubulin appears to be prevented from adopting its normal conformation by the bonds formed with its neighboring subunits in adjacent protofilaments. When MTs depolymerize, these constraining bonds dissociate and the shortening MT end is now terminated by a splay of protofilaments which bend by about 22° with every tubulin dimer in the chain.[66] This shape is commonly interpreted as a reflection of the minimum energy shape of GDP-tubulin dimers, and the resulting protofilament curling has been suggested to be capable of delivering a power stroke,[67] much like the work-producing segment of the adenosine triphosphatase cycle of a motor enzyme.[68]

4.7.3.6   Bending MT Protofilaments Can Exert Powerful Strokes

These features of tubulin polymerization dynamics suggest an alternative mechanism for the motion of particles in the previously described polymer-particle system. If the end subunit(s) of the polymer (a bending protofilament which can

provide a 'power stroke') pushes directly on the end-associated particle, forcing it to move forward (**Figure 2(i)**), a different mechanism for depolymerization-dependent force generation is identified. Here, the system does not have to wait for thermal fluctuations to help the particle overcome the force field of an opposing load. In contrast with the biased-diffusion mechanism, the power-stroke mechanism uses chemical energy stored in the MT lattice to produce useful mechanical work (**Figure 2(i)**). This 'forced-walk' mechanism,[69] in principle, allows the entire energy of the push to be converted into useful work for carrying the load. If we assume that the bending always takes place before the monomer or particle (serving as the coupler for a load) dissociates from the polymer tip, loads are carried processively (i.e., without detachment), and even nondiffusing couplers can do this job. Although such a scenario seems a priori farfetched, recent studies make it exceedingly likely that MT depolymerization generates pulling forces by a mechanism much like this. A direct demonstration of forces from bending protofilaments has been achieved by stably attaching a microbead to an MT wall, then inducing MT depolymerization (Section 4.7.4.2). As the MT shortened, the bead moved slightly in the direction of MT shortening, just as expected from the shape of curving protofilaments.[70]

One can estimate the maximum force which a disassembling MT can develop by assuming that all the energy from hydrolyzed GTP ($\sim 12\ k_BT$) is first stored in the strained conformations of GDP-tubulins in the MT wall, then all this energy is converted into a cargo's motion. For an MT with 13 protofilaments, the most common configuration of MTs in cells, the thermodynamic maximum is about 80 pN.[27] In a micro world, this is a very impressive value. It far exceeds the force required to move a mammalian chromosome through a cytoplasm, and may explain the startling observation that this motion is not blocked by the experimental application of hundreds of pico-Newtons.[27,47] In the following section, the authors explore the molecular and mechanical details of protofilament power strokes and review experimental measurement of the depolymerization-dependent forces exerted on an MT-attached bead.

4.7.4 Theoretical and Experimental Analysis of an MT Depolymerization Motor

Methods to study forces developed by shortening MT ends *in vitro* are similar to those used to study MT pushing. The significant difference, however, is that for depolymerization-dependent force generation, it is not possible to extract relevant information from a visual observation of polymer bending (e.g., as it pushes against a barrier). To study force generation by a disassembling MT, one must somehow couple a load to the MT tip. This has been difficult to achieve, slowing progress in this area. Recently, however, there have been significant advances in measuring depolymerization forces. The interpretation of these results would not have been possible without rigorous theoretical modeling of general properties of the MT depolymerization motor, as well as of the specific aspects of the experimental approaches used. The corresponding studies are reviewed in the following sections.

4.7.4.1 A Molecular-Mechanical Model of Depolymerizing MTs

A realistic model of disassembling MTs should include an explicit description of the changes in tubulin conformation which accompany the hydrolysis of β-tubulin-bound GTP. In the most comprehensive model so far, each tubulin monomer is described as a solid object which interacts with its lateral and head-to-tail neighbors (**Figure 3(a)**).[26,69] The structural transformation in tubulin which results from GTP hydrolysis is described as a bending moment, defined relative to the equilibrium angle χ_o which GDP-tubulin monomers form in curved protofilaments at the ends of MTs depolymerizing *in vitro*:

$$g(\chi) = 1/2B(\chi - \chi_o)^2 \qquad [8]$$

where $g(\chi)$ is the energy of the longitudinal interactions between head-to-tail monomers, which form the angle χ, and B is a coefficient which characterizes the flexural rigidity of the protofilament and corresponds to the bending stiffness of the longitudinal bond (**Figure 3(b)**).

The energy of lateral interactions $v(r)$ between tubulins in the MT wall is described with an activation energy barrier. Such a function allows the model to emulate the rupture of lateral bonds during protofilament curling:

$$v(r) = A\left(\frac{r}{r_o}\right)^2 e^{-\frac{r}{r_o}} \qquad [9]$$

where r is the distance between two interacting points on neighboring tubulins, A is a coefficient which describes the activation energy for lateral bond breakage, and r_o characterizes the length of the lateral bond (**Figure 3(b)**).

To model an MT, solid objects with the size of tubulin molecules and displaying these interaction energies are combined in the configuration of a 13-protofilament helical polymer, one end of which is firmly fixed. The behavior of this ensemble can be analyzed using the Metropolis method for Monte Carlo simulation.[71] One can show that, in this cylindrical configuration, each linear chain of solid bars which tend to bend (like GDP-tubulins) can be prevented from doing so simply by the action of the two terminal subunits (representations of a GTP-tubulin cap), which are assumed to have a smaller equilibrium bending angle than the GDP-tubulin and the same (or stronger) lateral bonds. This is true for a chain of any length and for any strength of lateral interactions between the GDP-tubulins, because the bending moments acting at the two ends of each bar in the linear chain which is 'capped' with terminal GTP-tubulins are compensated, so the lateral bonds in the GDP-containing part of the MT cylinder are not stressed.[26] If the restraining GTP-tubulin cap is removed, however, each chain of bars in the MT begins to bend outward, first stretching and then breaking its bonds with lateral neighbors. This process gives rise to the 'ram's horns', which are typical of a shortening MT end *in vitro*.

The configurations for GDP-containing polymers, which were calculated based on this model, are likely to capture the main features of a real disassembling MT in the presence of thermal noise (Video 1). Indeed, the same model (and with
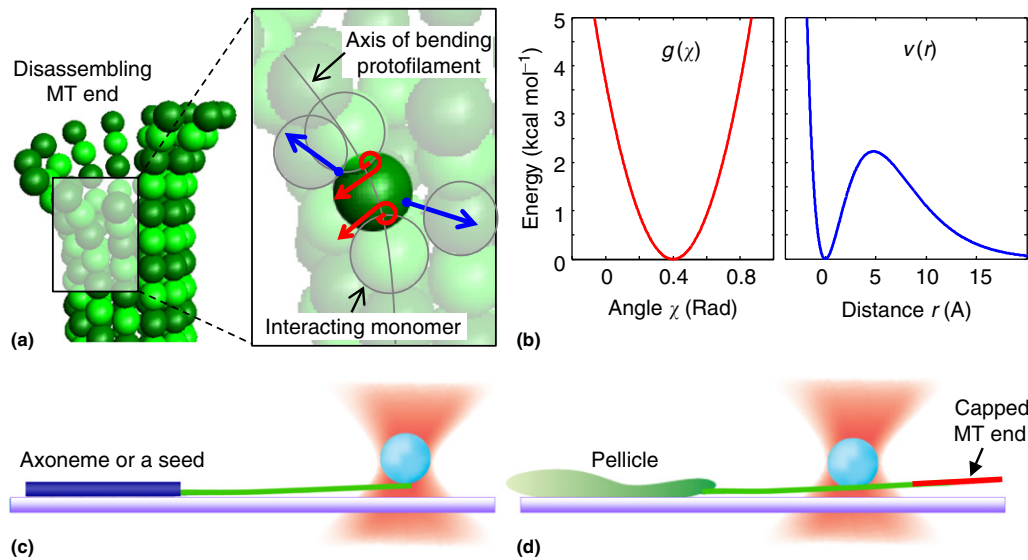
Figure 3 Theoretical and experimental analysis of a depolymerization motor. (a) Depolymerizing microtubule (MT) tip, drawn based on our mathematical model. The insert shows forces acting on a tubulin monomer (bright green) from its four neighboring subunits (gray perimeter) in the MT wall. At the shortening end, lateral contacts become stretched (blue arrows) and head-to-tail attached neighbors within same protofilament exert bending moments in opposite directions (bent red arrows). (b) Energy functions for longitudinal, $g(\chi)$, and lateral, $v(r)$, interactions between neighboring, guanosine diphosphate (GDP)-containing monomers. Angle χ describes bending between dimers within the same protofilament, whereas r is the distance between interacting dimers in adjacent protofilaments. Reproduced from Figure 2 in Molodtsov, M. I.; Ermakova, E. A.; Shnol, E. E.; Grishchuk, E. L.; McIntosh, J. R.; Ataullakhanov, F. I. A molecular-mechanical model of the microtubule. *Biophys. J.* **2005**, *88*, 3167–3179. (c) Schematic of the experimental approach (not to scale) used to study interactions between a protein-coated bead and a dynamic MT end. Proteins conjugated to the bead's surface enable bead motion with the MT end which switches stochastically between states of polymerization and depolymerization. Reproduced from Figure 3 in Franck, A. D.; Powers, A. F.; Gestaut, D. R.; Davis, T. N.; Asbury, C. L. Direct physical study of kinetochore-microtubule interactions by reconstitution and interrogation with an optical force clamp. *Methods* **2010**, *51*, 242–250. (d) Schematic of an experimental approach (not to scale) used to study interaction between a protein-coated bead and a disassembling MT end. Initially, the bead is attached laterally to the GDP-containing tubulins in the MT wall (green segment). MT depolymerization is induced by photoablation of the rhodamine-labeled, GMPCPP-containing MT cap (red segment). Reproduced from Grishchuk, E. L.; Molodtsov, M. I.; Ataullakhanov, F. I.; McIntosh, J. R. Force production by disassembling microtubules. *Nature* **2005**, *438*, 384–388. Copyright by Nature.

the same set of parameters) satisfies the experimentally determined temperature dependence of the depolymerization rate,[72] and can describe (1) the stability of a GDP polymer capped by a small GTP-cap[26] and (2) the results of experiments with depolymerizing MTs exerting forces on microbeads that are attached to MTs via various protein couplers (described later).[69,73]

The online version of this chapter contains Video **1**. The online version can be found at doi:10.1016/B978-0-08-095718-0.00409-0.

Although this model has some simplifications and shortfalls (e.g., it does not include the kinetics of tubulin assembly or of longitudinal bond breaking), it has proved to be a powerful tool for analyzing the power strokes of bending protofilaments. Two model conclusions are especially relevant. First, because protofilaments lose their lateral association concomitantly with bending, each protofilament can develop an independent power stroke. Therefore, these forces are additive, so the depolymerization force from the whole MT should be roughly 13 times larger than the force from one protofilament. Second, the maximum force which can be generated under optimal conditions by one bending protofilament in this model is almost 6 pN, very close to the upper limit imposed by the chemical energy available from GTP hydrolysis.[27] This value is similar to the force which can be

developed by ATP-dependent motor enzymes, such as kinesin. If all MT protofilaments were to work in concert, the depolymerization-dependent force of a single MT could be up to 13 times greater than the force developed by a single ATP-dependent motor.

4.7.4.2   Experimental Approaches to Measuring the Depolymerization-Dependent Force

The most common experimental way to attach a 'load' to the shortening MT tip has been with the help of various MAPs. When analyzing these experimental results one must then keep in mind that MAPs are known to affect the dynamics of tubulin assembly/disassembly. Furthermore, to draw quantitative conclusions, it is imperative to know exactly how, the coupling is achieved, whether it involves all or only some of the protofilaments, and where, the forces are being applied and measured. So far, three experimental approaches have been used to study the interactions between a shortening MT tip and its attached load. The setup which is closest to the one used to examine pushing forces involves only a single modification – the tip of the MT, growing from a bead-associated seed, comes in contact with a wall coated with an MT-interacting protein. When the minus-end-directed motor, dynein,

was used with this method, MTs interacting with such a coated wall behaved very differently from those encountering a wall with no coating.[73] When the MTs are shrinking and ATP is present, there is a pull on the bead-attached MTs, but the interpretation of these force-generating events is not straightforward. Dynein may be contributing as a motor, not just a coupling factor, and the relative roles of the two kinds of mechanochemistry have not yet been sorted out.

The second method for this study has been a modification of the experimental system originally developed by Coue et al.[29] They used *Tetrahymena* 'pellicles' (lysed and deciliated protozoans), that were bound to the coverslip in a microscope chamber. Such pellicles define the orientation of the MTs which grow from them; the fast-growing or 'plus' ends are distal, just like in mitotic spindles. Coverslip-adhered pellicles also provide a firm anchorage for the MT minus ends, so pulling forces can be examined. Dense MTs arrays were grown from the pellicles using purified tubulin in the presence of GTP; MT depolymerization was initiated by washing away soluble tubulin. This approach has helped to show that isolated mammalian chromosomes and vesicles, as well as microbeads coated with various motors, bind these MTs and move toward the pellicles in an ATP-independent, depolymerization-dependent manner.[29,30] This was the first direct demonstration that depolymerization could actually generate force; it had a significant impact on this field, but the exact mechanism for the motion of these objects is still unknown.

More recently, Asbury and colleagues[74] advanced this approach by using coverslip-attached, stabilized MT seeds which nucleated single MTs. Beads coated with various non-motor MAPs were brought in contact with the tips of these MTs using laser tweezers (**Figure 3(c)**)[74]. Certain MAPs provided specific attachment to the MT ends and enabled the beads to 'ride' with the growing tip, even when the laser tweezers were used to pull the beads away from the tip (0.5–3-pN force).[37,75] Occasionally, the MT with the riding bead underwent a catastrophe (i.e., it abruptly began to disassemble), and some of the trapped beads reversed their direction of motion. In the absence of load, they traveled with the shortening ends relatively far, as in the original observations by Lombillo et al.[30] However, when a load was applied, these runs shortened and the beads usually traveled less than a micron.[37,75] Similar motions were seen using beads coated with either of two kinetochore complexes, Dam1 and Ndc80, although the mechanisms proposed for MT coupling by these proteins were widely different.[37,75] Clearly, the readout from this experimental system reflects not only the ability of the MT to pull, but also the properties of the coupling protein, which are not yet known in full (see Section 4.7.5). Together, these experiments suggest that the depolymerization motor can generate a force of at least 10 pN.[76]

The most straightforward approach to studying the depolymerization-dependent force so far published reduced the uncertainties which arise from coupling to an MT tip via multicomponent MAP complexes. Instead, the bead was attached directly to the MT wall via the well-studied and highly stable biotin-streptavidin link (**Figure 3(d)**). MTs were then induced to depolymerize by ablating a photolabile cap from the MT end.[77] In this experimental system, the streptavidin-coated beads were completely immobile until MT depolymerization was triggered. Not surprisingly, the beads failed to move processively with the shortening MT ends, even in the absence of the load. However, as the MT depolymerized, the beads frequently showed a small jerk in the direction of depolymerization prior to their detachment. Because this experimental system contains no soluble proteins, no bead-associated MAPs, and no soluble nucleotides, the pull must have been generated by conformational changes which took place at the shortening MT end as it passed by the bead (**Figure 4(a)**[43,70]). This 'single-shot' force, as measured by following the motion of the associated bead in a stationary laser trap, was very small – barely reaching 0.5 pN. The simplicity of this experimental system, however, has allowed a deep insight into the underlying mechanisms. Next, the authors consider the mechanics of this system in more detail. By taking advantage of the molecular-mechanical MT model, the authors arrive at the nonintuitive conclusion that this measured force amplitude corresponds to the action of a very efficient and powerful depolymerization-dependent motor.

4.7.4.3 Mechanics of Protofilament Bending and Interaction with an Attached Microbead

Two geometric objects, a 1-μm sphere and a 25-nm cylinder, can make lateral contact at only a geometric point. In a realistic case, like an MT and a protein-coated bead, the contact area is larger, given that MT binding may stretch the protein coat on the bead. Calculations suggest that even in this case, however, a streptavidin-coated bead can only bind to three to eight head-to-tail tubulin dimers along the length of one or two adjacent protofilaments.[70] The MT model can then be used to describe the behavior of such a system, while taking into consideration the mechanical action of an immobile optical trap which acts at the center of the bead to resist its motion (for more details see Grishchuk et al.[70]). The bead's position is then described by an equation of motion in the general form

$$m\frac{d^2\mathbf{r}}{dt^2} + \gamma\frac{d\mathbf{r}}{dt} = -\partial U/\partial\mathbf{r} + \mathbf{F}(t) \qquad [10]$$

where U is the potential energy of the full system consisting of the MT bound to the bead in the force field of the optical trap, m is the bead's mass, γ is its viscous drag coefficient, and $\mathbf{r}$ describes the vector displacement of the center of the bead. The function $\mathbf{F}(t)$ describes the force causing Brownian fluctuations. Depolymerization of MTs is a relatively slow process (10–500 nm s^{-1}), so all accelerations in this system can be neglected. For the typical rates of MT disassembly, the second term on the left side in eqn [10] is also three orders of magnitude smaller than the developed forces. Furthermore, for millisecond and longer processes, $\langle\mathbf{F}(t)\rangle = 0$. Thus, bead position is fully determined by the equation

$$\partial U/\partial\mathbf{r} = 0 \qquad [11]$$

and hence simply by the balance of all applied forces.

For simplicity, the authors consider the mechanics of this system while assuming that the bead is attached laterally to only one protofilament in the MT wall. The bead's diameter
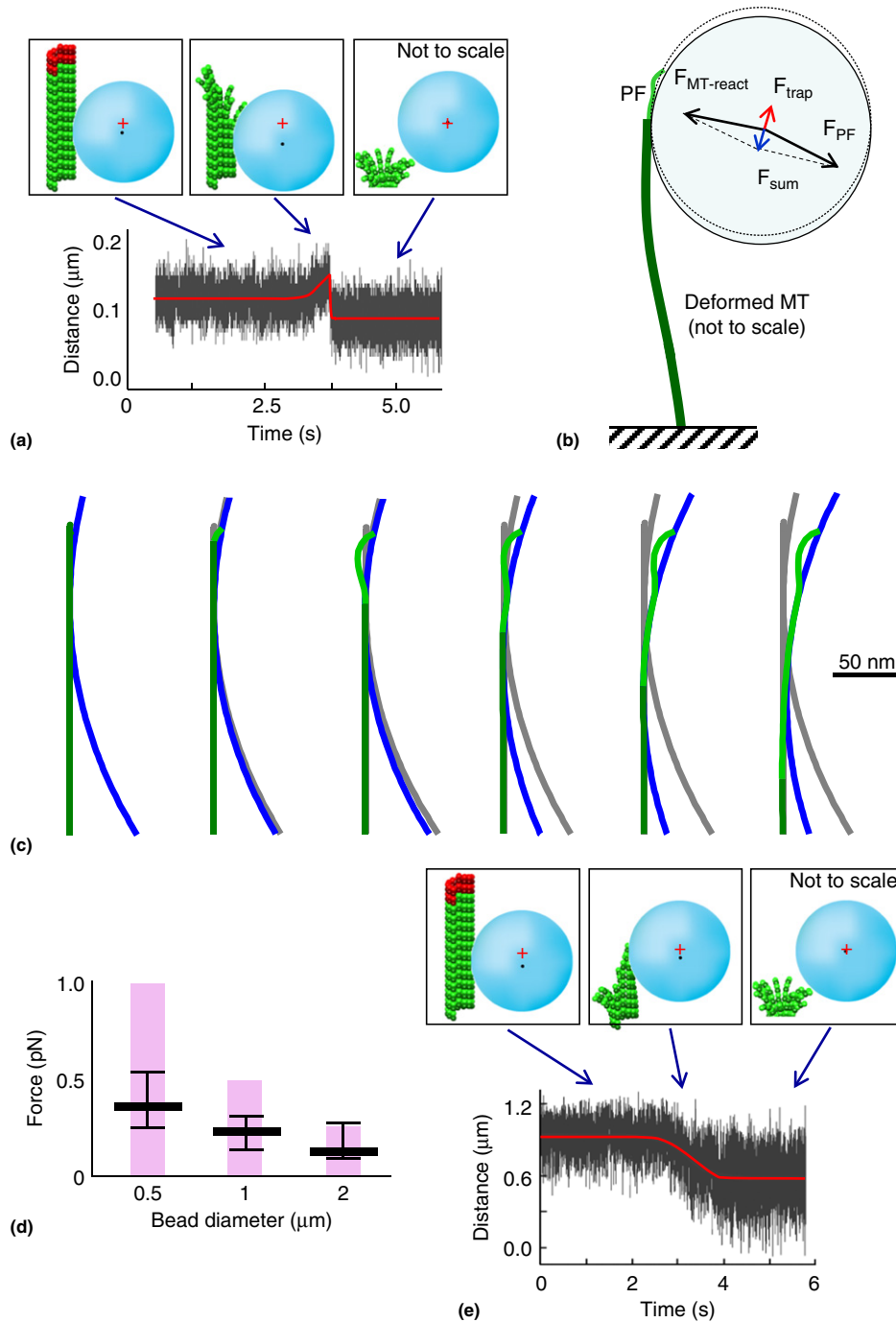
Figure 4 Mechanics of protofilament (PF) bending. (a) The graph shows the experimental signal recorded on a quadrant photodetector from a streptavidin-coated bead and a depolymerizing biotinylated microtubule (MT). Bead position oscillates rapidly (black curve) as a result of thermal noise (red curve is average position). Diagrams above the signal illustrate interpretations. Initially, the bead (not to scale) is attached to a stable MT wall and is under a small trapping force, so the center of a bead (black dot) is shifted from the trap's center (red cross). At the end of experiment, the MT has depolymerized and the bead has separated from the MT; the average noise of such an MT-free, but still trapped, bead is slightly bigger, and the bead is now located at the trap's center. The transition between these states contains a fast spike – the bead moved away from the trap's center under the force of bending protofilaments. Then its associated tubulins detached from the MT end, and the bead abruptly fell into the center of the trap. (b) Forces acting on a protofilament-associated bead. The initial position of a bead attached to the intact MT is shown with dashed lines. Subsequently, the bead shifts (solid contour) while rotating around its attachment site. See text for other details. (c) Calculated configurations of a bead (blue contour) and depolymerizing MT (green; still frames from Video 2). When the MT begins to shorten, the bead-associated tubulin subunits (light green) bend and rotate the bead slightly. Gray contours show the initial system configuration. (d) The force measured at the center of a bead depends on the bead's diameter. Symbols correspond to experimental signals (mean with interquartile range). Data from Grishchuk et al.[43] Purple bars depict a range of force amplitudes predicted by the model. Maximal force is achieved when the bending of a bead-associated protofilament is unrestricted by the adjacent protofilaments; all other scenarios lead to attenuated force.[70] (e) Example of an experimental signal which demonstrates the flaccidity of protofilament protrusions. Under the trapping force, protofilaments may bend in the direction opposite to that dictated by their natural curvature.

(1000 nm) is much larger than the linear region of bead attachment (20–60 nm). When depolymerization starts, the lateral bonds between adjacent protofilaments break apart and GDP-containing tubulin dimers begin to bend toward their minimum energy configuration. The local curvature of the fully bent GDP-containing protofilament is significantly larger than that of the bead, where curvatures are defined as the reciprocals of the radii of best-fit circles for these shapes. The bead's surface therefore prevents the attached protofilament from reaching its equilibrium configuration, and the force from bending dimers, F_{PF}, pushes on the bead in a direction primarily perpendicular to the MT axis (**Figure 4(b)**). Because the bead is placed in the force field of a focused laser beam, it also experiences a restoring force from the trap, F_{trap}. An MT has inherent, albeit small, flexibility, so when the trap pulls on the bead it deforms the MT (**Figure 4(b)**). The bead-attached protofilament also deforms under the action of the trapping force. The elastic forces arising from these deformations, as well as from stretching of the biotin-streptavidin bonds between the protofilament and its attached bead, leads to $F_{MT\text{-}react}$. At steady state, the vector sum of $F_{MT\text{-}react}$ and F_{PF} acts mostly along the MT axis and in a direction away from the disassembling tip (F_{sum}; **Figure 4(b)**).

Figure 4(c) shows a time-lapse sequence from Video 2, which contains calculated MT-bead configurations in this system.[70] It is easy to see that because the bead is stably attached to the protofilament, it cannot move along its surface. Instead, the bead rotates slightly while the system moves to its steady-state configuration (**Figure 4(c)**). Calculations show that the balance is achieved with a very small bead displacement in a direction perpendicular to the MT axis (about 7 nm for a 5500-nm-long MT with a 1000-nm diameter bead and a trap stiffness of 0.01 pN nm^{-1}). The bead's displacement along the MT axis is somewhat larger (50–60 nm for these parameter values), and is achieved when the MT-parallel components of F_{trap} and F_{sum} are balanced. The magnitude of force measured in the experiment (the MT-parallel component of F_{trap}; **Figure 4(b)**) is significantly smaller than the force F_{PF} with which the protofilament is pushing on the bead. This mechanical interpretation is supported by experimental observation that larger forces are measured in the same experiment when smaller beads are used,[43] just as predicted by this model (**Figure 4(d)**). Calculations show that a single protofilament pushing on the attached bead with about 5.8 pN force displaces a 1-μm bead in a laser force field to the distance which corresponds to a 0.5-pN trapping force. This value is in excellent agreement with the magnitude of forces measured in the experiments with streptavidin-coated beads (maximum force measured was 0.45 pN).[70] Therefore, when the 'lever arm' effect is taken into account, these experimental results imply that the force developed by a bending protofilament in this experimental system is about 5.2 pN, that is only 1 pN less than the thermodynamic maximum.[27]

The online version of this chapter contains Video 2. The online version can be found at doi:10.1016/B978-0-08-095718-0.00409-0.

It is interesting to compare this mechanical system with forces which act on a bead of 1 μm in diameter and which is carried by a kinesin motor along a coverslip-attached MT. These MT-dependent motility systems bear some similarities;

for example, in both, the bead is attached to the MT with protein links which have a similar characteristic size. Also, as with depolymerization-dependent motion, the kinesin-based system is relatively static, and the terms for acceleration and viscous drag can be ignored. However, these motility systems have different geometric properties, because kinesin moves on an MT which does not disassemble. As kinesin starts walking, it exerts a force at the bead's surface in the direction of the motor's movement, while the trapping force is applied at the center of the bead. Together, these forces create a torque which rotates the bead and pushes it against the MT wall. This pushing force, however, is compensated by elastic forces from the MT, and if the bead's friction on the MT is negligible, a steady-state is achieved in which the force developed by the kinesin is equal to the counteracting trapping force. With protofilament power strokes, however, the geometry of the system is more complex, and it differs for different modes of coupling the cargo to the MT end. To avoid misinterpretations, the corresponding mechanics should be analyzed for each experimental system and mode of attachment.

4.7.4.4 Effect of an Opposing Load on Protofilament Bending and MT Disassembly

Further details of bead-MT interaction can be learned by analyzing the kinetics of bead motion under the action of a depolymerization force. Soon after MT depolymerization is triggered, the streptavidin-coated bead begins to move toward the stably attached MT minus end, that takes it away from the center of the laser trap (**Figure 4(a)**). This motion can be followed with nanometer precision by imaging the bead on a quadrant photodetector. The kinetics of changes in the bead's coordinates should then provide information about the rate with which the bead-bound protofilaments generate force. If this interpretation is correct, the characteristic time for this motion should correspond to the rate with which the MT disassembles. This expectation was evaluated by using the buffers with various concentrations of Mg^{2+} ions, because the rate of MT depolymerization is known to depend on Mg^{2+}; at higher Mg^{2+} concentrations, MTs disassemble faster.[78] Indeed, the characteristic time for the rising part of the force signal decreased with increasing Mg^{2+} concentration,[70] as one would expect.

This system can then be used to analyze how protofilaments bend in the presence of a restraining force. There is great interest in how an opposing load affects tubulin kinetics at a disassembling MT end. During metaphase of cell division, the duplicated chromosomes frequently show complex motions in which attached sister chromatids move together, while one is bound to MTs associated with one pole and the other to the opposite pole. The duplicated chromosome stays coupled to MTs, even when under tension, but an increase in tension can induce MTs to switch from a depolymerizing state to a polymerizing one.[79] The mechanism of this switching is not known. It may involve some complex regulatory reactions (e.g., those based on protein phosphorylation). Alternatively, it has been proposed that this behavior might arise if a high load constrains protofilament bending, thereby promoting MT rescue and polymerization.[80,81] Analysis of changes in

the position of streptavidin-coated beads, which moved under the opposing forces of a laser trap, have provided some insight into this potentially significant phenomenon, as described next.

In the experimental system which uses MTs with photolabile caps, soluble tubulin is absent, so an MT disassembling under load cannot possibly switch to polymerization, even if the previous hypothesis is true. Instead, this experimental approach allows one to examine the time it takes the streptavidin-coated bead to transit to the center of the laser trap as the depolymerization wave passes by. After the dissolution of a longitudinal tubulin-tubulin bond downstream from the bead, the bead loses its connection with the MT and jumps abruptly to the optical center of the laser trap (<1 ms). Such events have, indeed, been observed (**Figure 4(a)**). However, about half the beads studied moved to the center of the trap much more slowly, with an average time of ~ 800 ms.[70] The most likely explanation for this slower kinetics of bead motion is that these beads were not completely free; they were moving under the action of the trap while still linked to the disintegrating MT (**Figure 4(e)**). Mathematical modeling of the bead-MT system predicts that under the force field of the laser trap, the bead will begin to move toward the center of the trap before it completely loses its attachment, causing the flaccid protofilaments, which remain in the partially depolymerized MT, to bend in the direction opposite to that dictated by the natural bending of GDP-tubulin. This transition time, therefore, characterizes tubulin's dissociation from protofilament tips which are straightened by an opposing force. It might be expected that increased pulling on such protofilaments might promote the dissolution of their longitudinal tubulin bonds, but the experiment showed an opposite trend.[70] Thus, current evidence suggests that the rate of tubulin dissociation is strain dependent, such that any tension which slows the rate of protofilament relaxation to its minimum energy shape inhibits tubulin disassembly.

4.7.4.5   MT Dynamics under a Continuous Force

A strain dependence of the dissociation rate for head-to-tail attached tubulins has also been suggested by the work of Franck et al.[82] They studied motions of beads coated with the kinetochore-associated complex Dam1, applying controlled forces to the bead with a laser force clamp. Dam1-coated beads formed attachments to the plus ends of growing MTs, and when these polymers switched stochastically into a depolymerization state, the beads moved while hanging on to the shortening MT ends. Consistent with the results from streptavidin-coated beads, loads applied through the Dam1-coated beads slowed MT depolymerization (a change of about 40 nm s^{-1} per 1-pN load). Furthermore, by carrying out these experiments in the presence of soluble tubulin, the authors were able to observe an increased probability of depolymerization rescue with a larger load, just as expected from live observations and micromanipulation studies with dividing cells.[79]

An assisting force, applied to Dam1-coated beads in the direction of their motion with MT growth, did not increase the rate of tubulin polymerization, but it did inhibit catastrophes (a approximate threefold decrease for a 2-pN load vs. a 0.5-pN load). Under opposite mechanical conditions (i.e., when a growing MT tip was compressed), the MT was more likely to undergo a catastrophe, an effect which was proposed to result from a reduced rate of tubulin addition at the compressed tip.[20] In contrast, Franck et al.[82] suggested that the ability of the pulling force to inhibit catastrophes at the growing MT tip was not caused by an increased rate of tubulin assembly, but had its roots in the effect of tension on protofilament behavior. However, the mechanism of this effect on these bead motions, and how these beads bind to the MT tip, is not yet known. Further progress in specifying these interrelationships requires continued rigorous theoretical analysis and experimental testing. Determining and controlling the exact mode of the bead's attachment to and interaction with the MT wall and bending protofilaments remain the most challenging aspect of this area of research. The following sections look more deeply at macromolecular MT-tip couplers and their characteristic features.

4.7.5   Molecular Devices to Couple MT Depolymerization to Processive Cargo Motion

As described earlier, MT depolymerization plays a pivotal role in one of the fundamental processes of life – chromosome segregation during cell division. Mitotic chromosomes bind to the ends of MTs with the help of a specialized proteinaceous structure, the kinetochore. During cell division, chromosomes move at the ends of depolymerizing MTs without losing their attachments. Moreover, it is well established that in many cell types, MTs shorten from their kinetochore-attached ends.[83] Together with the finding that MT depolymerization can transport the chromosomes, these features of chromosome motion imply that kinetochore-associated proteins provide a coupling between a chromosome and the shortening MT tips which can (1) capture the energy from MT depolymerization and (2) ensure the stability of the attachment under large and variable loads. Thus, the authors define a kinetochore coupler as a macromolecular device which serves to achieve these specific goals. A coupler or its parts might also be involved in other kinetochore functions, such as error correction and corresponding signaling.[84] It is not yet known if and how these diverse functions are integrated together with the coupling mechanisms, so this aspect of kinetochore functioning will not be discussed. Here, the authors focus on specifying the principal features of theoretically possible couplers, as well as on reviewing the progress in quantitative analysis of the candidate, multiprotein kinetochore complexes.

4.7.5.1   The Famous Hill's Sleeve

Terrell Leslie Hill would have been famous for his outstanding contributions to theoretical sciences even if he had not invented the first explicit description of a kinetochore-MT coupling device.[45] This coupler, usually referred to as 'Hill's sleeve', made a big impact on researchers of mitosis, and the corresponding publication in 1985 is an obligatory citation in any current review on this subject. This theoretical model, based on the classic idea of biased diffusion, was very

influential, in part because it was both specific and quantitative. Hill[45] thoroughly described the design of the sleeve he had in mind and demonstrated that for reasonable values of model parameters, this coupler could achieve the previously specified biological goals – a fundamental discovery. A brief summary of the model's features and parameters are as follows.

The sleeve designed by Hill is a rigid, narrow tube which is only slightly wider than an MT, and is about 40 nm long (Figure 5(a)). One might wonder about the likelihood that the tip of a growing spindle MT would find such a narrow channel, but Hill[45] calculated that this would not be an improbable event. However, subsequent work by others demonstrated that to capture all 46 chromosomes (as in human cells) in a reasonable time, some additional assumptions about MT-chromosome interactions must be introduced.[85] A 40-nm-long channel spans approximately five tubulin dimers in a single protofilament, but with a 13-protofilament MT, the sleeve can interact with as many as 65 dimers. The inside of Hill's sleeve was lined with MT-binding proteins; in the published model, the number of such MAPs was also 65. Hill also specified that the distance between adjacent sites for MAP-tubulin binding should be 6.15 Å. It followed that either each tubulin dimer or the MAP had 13 binding sites along its length, not an entirely reasonable model assumption (for an alternative supposition concerning this very small step size, see Supplement 2 in Ref. 27). The key feature of the MAP in Hill's sleeve is that it can undergo one-dimensional diffusion on the MT's surface, just like the particle considered in Section 4.7.3. There, the authors assumed that the particle could not detach from the MT surface. In Hill's model, this assumption is a natural consequence of the sleeve's design, because the position of each MAP is fixed within the rigid framework of the sleeve. Being tied to a rigid cylinder, the individual MAPs cannot move away from the MT surface, even as they undergo cycles of detachment and reattachment during their one-dimensional diffusion, while hopping from one binding site on the MT surface to the next. This model feature has a pronounced impact on the energetics of MAP-MT interaction. The coupler's structure effectively lowers the energy barriers for MAPs detachment during its diffusion (parameter b), relative to the energy barrier the MAP must overcome to separate completely from a tubulin at the MT end (parameter w; Figure 5(b), (c)). Furthermore, each MAP can move only in synchrony with the other 64 binding proteins in the coupler – a specific and unique characteristic of this coupler.

Such an ensemble of MAPs, when brought in contact with an MT end, moves with the sleeve as a whole, exhibiting biased diffusion toward the position which gives a larger overlap with the MT surface. A fuller insertion corresponds to more MAP-tubulin bonds, hence to a lower free energy of the sleeve-MT interaction (Figure 5(c)). A molecular 'roughness' of MAP-MT interaction, embodied by the parameter b, would, however, prevent a complete insertion, and the sleeve would find its dynamic steady-state position with some intermediate degree of MT overlap. It is easy to see that if the MT end which is inserted in this sleeve begins to shorten, it biases the coupler's diffusion. The sleeve and its attached chromosome will follow the shortening end, while trying to restore the overlap with reduced binding energy.[46] For a known rate of chromosome motion (about 1 μm min⁻¹), chromosome diffusion properties, and sleeve's geometric structure, Hill determined energy parameters b and w (0.3 k_BT and 2.5 k_BT, respectively). Such a coupler can carry a relatively wide range of loads at a constant speed. The latter feature echoes the force-velocity relationship measured for chromosomes in grasshopper spermatocytes, where the velocity began to drop only with very high loads
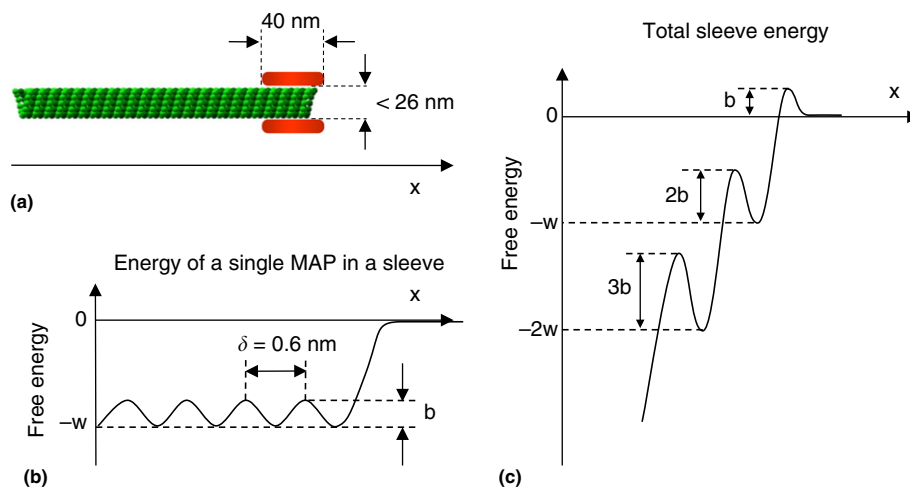
Figure 5 Energy of interactions in Hill's sleeve model. (a) Diagram of the coupler, a narrow cylinder which can undergo biased diffusion coupled with a dynamic microtubule (MT) end. (b) In general, energy of the protein's site-specific binding should be the same for all subunits of the polymer terminal or not. In rigid Hill's structure, however, the energy barrier for MT-associated protein (MAP) transitions from one binding site to the next is lower, relative to the binding energy at the terminal site. (c) The sleeve diffuses on an MT surface by synchronously moving all its binding elements. Larger sleeve-MT overlap corresponds to a lower free energy, but it requires more energy for transitions. Adapted from Hill, T. L. Theoretical problems related to the attachment of microtubules to kinetochores. *Proc. Natl. Acad. Sci. USA.* **1985**, *82*, 4404–4408. Copyright by PNAS.

(about 100 pN; the load per one MT is, of course, smaller, because these kinetochores bind many MTs).[47] In Hill's model, however, the overlap between the sleeve and the MT shortens with increasing load until the sleeve finally detaches at 9 to 15 pN load per MT.[46] Thus, the sleeve is not very efficient in converting the energy available from MT disassembly into productive work, consistent with the authors' general conclusion in Section 4.7.3 about this property of the biased diffusion-based couplings.

There is still a significant interest in the sleeve model for chromosome coupling, even though the most recent and thorough ultrastructural studies of MT-kinetochore interfaces have failed to identify such a structure.[86–88] Furthermore, the mechanochemical pathway for MT disassembly (Section 4.7.3.5), that came to light after Hill's model was published, makes highly improbable Hill's assumption that tubulins can dissociate in a narrow sleeve without protofilament bending. Moreover, the ends of MTs embedded in a kinetochore, as seen by electron microscopy, are rarely blunt.[87] They show a flared morphology, that is simply inconsistent with a sleeve-based coupling,[27] although there is a recent theoretical attempt to reconcile this contradiction by designing a sleeve with a more complex geometry.[88] In the authors' view, however, the structural findings make it highly unlikely that a coupler with characteristics proposed by Hill is involved in the motion of eukaryotic chromosomes. Nonetheless, Hill's powerful contribution continues to promote interest in the biased-diffusion mechanism for the motion of these molecules and their assemblies. When using Hill's legacy, however, it is important to remember that the ability of his sleeve to couple shortening MTs to their cargo was obtained through a model with very specific assumptions and parameter values. Although biased diffusion probably plays important roles in some MT-dependent motions, their analysis cannot be carried out simply by applying the equations Hill wrote for a sleeve. This is true even for a geometrically similar coupler (e.g., a planar ring that is one subunit thick).

4.7.5.2 A Wide Ring with Flexible Radial Spokes Can Capture the Energy from Bending Protofilaments Efficiently

A ring-shaped coupler was proposed by Koshland et al.[67] in 1988 based on their discovery that MTs shortening *in vitro* could retain an association with kinetochores on immobilized chromosomes, and the earlier descriptions of ring- and spiral-shaped oligomers of tubulin, which form under certain conditions of MT depolymerization.[89] The first theoretical analysis of force transduction by a planar, rigid ring which does not bind the MT wall was carried out fairly recently, after the development of a quantitative molecular-mechanical model of MTs.[27] It was shown that a power-stroke mechanism can achieve the maximum utilization of the strain energy stored in an MT lattice, and hence can generate the strongest possible force, as long as the coupler does not restrict full dissociation of the lateral bonds between tubulin dimers (Figure 6(a)). This means that the ring must not have too small an inside diameter; its optimal value is 35 to 40 nm. For this reason, the power-stroke mechanism cannot work within the narrow sleeve postulated by Hill.[45]

Research on ring-shaped couplers gained momentum when the first kinetochore complex with this geometry was discovered. Both the Barnes/Drubin group, and the Harrison lab found that a multiprotein complex from budding yeast, called Dam1 (or DASH), assembles spontaneously into ~16 subunit rings around MTs.[90,91] The electron-dense core of a Dam1 ring is separated from the outer MT wall by a 3- to 6-nm gap – a distance very similar to a 5- to 7-nm gap predicted for an energy-efficient ring coupling. The typical distance for protein-protein interactions is, however, much shorter than the gap between the core of the Dam1 ring and the MT wall (Figure 6(a)). Thus, the finding that Dam1 ring subunits can bind to the MT wall directly led to the prediction that this ring's inner surface and the MT wall would be connected by protein linkages.[27] The subsequent ultrastructural studies by the Nogales and Harrison labs confirmed these expected structures (Figure 6(b)).[50,92] The modeling therefore suggests that the wide diameter serves to maximize the energy efficiency of Dam1 ring, whereas its radial spokes ensure adhesion to the MT wall.

Theory further emphasizes that the optimal performance by such a coupler will be achieved if the spokes are flexible, because stiff linkages effectively reduce the ring's diameter. This prediction has not yet been tested directly, although structural studies imply that the inward-directed protrusions in a Dam1 ring are not rigid.[92] Furthermore, the model's prediction that such spokes should promote certain preferred orientations of the Dam1 ring on the MT wall has been verified experimentally.[69] It is worth emphasizing that flexibility of the spokes enables their somewhat independent behavior, in contrast with Hill's sleeve, where all bonds between the MT and the coupler dissociated and reassociated in synchrony.

4.7.5.3 Biophysical Constraints on Processive Coupling by a Dam1-Like Ring

Just as Hill's sleeve has been an epitome for biased-diffusion mechanisms, the Dam1 ring has commonly been discussed in connection with protofilament power strokes. Modeling shows, however, that the mechanism of any ring's motion is not defined so much by its geometry as by the parameters which describe ring-MT binding. Depending on the strength of these bonds, the ring can move either by biased diffusion or by a forced walk and, indeed, even by a combination of these mechanisms.[69] If the energy with which each radial spoke binds to the MT wall is relatively low (< 5 k$_B$T), a ring with 13 such linkages will show one-dimensional diffusion on the MT wall. When the MT depolymerizes, the flared protofilaments may serve as a barrier, because their radial span is significantly larger than ring's diameter. In this case, the ring's thermal motions become biased (Video 3). Although, technically, these bending protofilaments push on the weakly bound ring when it comes in contact with them, when no load is present this aspect of their interactions is mechanically insignificant, because of the low resistance to ring sliding.

The online version of this chapter contains Video 3. The online version can be found at doi:10.1016/B978-0-08-095718-0.00409-0.

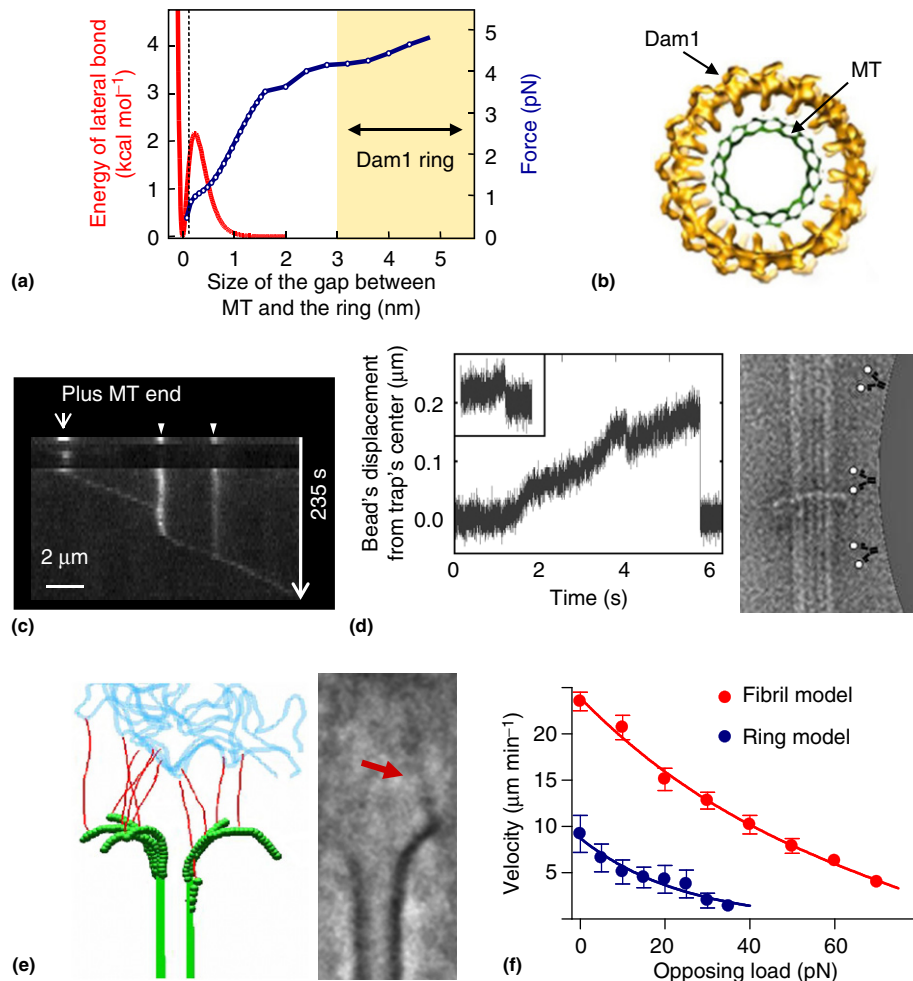This scenario seems to provide an excellent explanation for a ring-dependent chromosome coupling, but as with other

Figure 6 Biomechanical design of a Dam1 ring. (a) Theoretical prediction of the amplitude of force developed by a bending protofilament (blue curve) as a function of its distance to the fulcrum.[27] Larger force is exerted when the inner surface of the ring is farther from the outer surface of the microtubule (MT) (i.e., when the gap exceeds a typical distance for protein–protein interactions, as seen from an energy function [red curve]). (b) Cross section of a 16-protofilament MT densely decorated with Dam1 heterodecamers, as seen by helical reconstruction. Inward-directed protrusions are clearly visible. Adapted with permission from Wang, H. W.; Ramey, V. H.; Westermann, S.; Leschziner, A. E.; Welburn, J. P.; Nakajima, Y.; Drubin, D. G.; Barnes, G.; Nogales, E. Architecture of the Dam1 kinetochore ring complex and implications for microtubule-driven assembly and force-coupling mechanisms. *Nat. Struct. Mol. Biol.* **2007**, *14*, 721–726. Copyright by Nature. (c) Kymograph of Alexa488-labeled Dam1 on a depolymerizing MT. The majority of dots formed by wild-type Dam1 does not move until an MT end comes by (dots marked with arrowheads diffuse at less than $10^{-7}\ \mu m^2\ s^{-1}$). Under the depolymerization force, these dots move steadily but slowly (oblique line), indicating a relatively strong binding between the MT and the ring. Adapted with permission from Grishchuk, E. L.; Spiridonov, I. S.; Volkov, V. A.; Efremov, A.; Westermann, S.; Drubin, D.; Barnes, G.; Ataullakhanov, F. I.; McIntosh, J. R. Different assemblies of the DAM1 complex follow shortening microtubules by distinct mechanisms. *Proc. Natl. Acad. Sci. USA* **2008**, *105*, 6918–6923. Copyright by PNAS. (d) Quadrant photodetector record of the signal from a Dam1-coated bead moving under an MT depolymerization force in the presence of soluble Dam1. When the lever-arm effect is taken into account, the data suggest that the ring experiences on average 30-pN force in this system. The inset shows an analogous signal but from a streptavidin-coated bead that attaches laterally to the MT wall. The image at right illustrates a proposed ring-bead configuration. The Dam1 coat on a 500-nm bead is created with the help of Dam1-specific antibodies (drawing); the bead-associated Dam1 binds to the Dam1 ring which encircles the MT (negative staining imaged by electron microscopy). The encircling coupler transduces force from all protofilaments, while the 'streptavidinated' bead experiences a power stroke from only one to two protofilaments. (e) Reconstruction of anaphase kinetochore MT ends from a Potoroo Kidney cell line. Protofilaments are traced in green, kinetochore fibrils are in red, and a representation of chromatin is in blue. The micrograph is the average of multiple tomographic slices containing protofilaments with intermediate curvature which bend to the right. The red arrow points to a kinetochore fibril, that is attached to the averaged protofilament and extends toward the chromatin. (f) Theoretical predictions for force-velocity relationships for two couplers. A fibrillar coupler is more energy efficient than a Dam1-like ring; it is characterized by unretarded movement with no load and a larger maximal load. (e) and (f) Image from McIntosh, J. R.; Grishchuk, E. L.; Morphew, M. K.; Efremov, A. K.; Zhudenkov, K.; Volkov, V. A.; Cheeseman, I. M.; Desai, A.; Mastronarde, D. N.; Ataullakhanov, F. I. Fibrils connect microtubule tips with kinetochores: a mechanism to couple tubulin dynamics to chromosome motion. *Cell* **2008**, *135*, 322–333.

biased-diffusion mechanisms, the 'Achilles heel' of such a process lies in its behavior under load. First, as discussed in Section 4.7.3.3, thermal energy cannot support the transport of large loads at the end of a polymer which shortens at physiologically relevant rates. Second, a weakly bound ring is unlikely to fulfill one of the goals of chromosomal coupling – to maintain a stable attachment to a shortening MT end. For example, a binding energy of 3 k_BT per spoke cannot prevent detachment of a ring which forms 13 attachments to the MT wall when the load is more than 6 pN.[69] The authors conclude that such a mechanism for ring-dependent coupling is theoretically possible and may be an acceptable solution for MT-dependent transport in some biological systems, where slow kinetics of motion and/or large loads are not an issue. However, a weakly bound ring cannot maintain its attachment to an MT end under large and variable loads. During mitosis, the kinetochore may occasionally experience a large load; a variable load or some random event may pause depolymerization or may cause it to switch into growth. These conditions are likely to promote the loss of the protofilament flare and a straightening of the MT end (see Sections 4.7.4.4 and 4.7.4.5). At a blunt MT end, the weaker the ring's adhesion, the more readily it detaches.[69]

A higher stability of coupler attachment is obviously achieved if the ring binds more strongly to the MT wall. If the binding is excessively strong, however, even the powerful protofilament power strokes will no longer be able to move it along the MT wall, and the ring will block MT depolymerization. This consideration demonstrates the dichotomy of a ring-shaped coupling which arises from antagonistic requirements for the coupler's stability of attachment (higher binding energy) and for the coupler's sliding (lower binding energy). Theory helps to specify the range of ring affinity, that provides an acceptable compromise – 10 to 14 k_BT per bond.[69] At 13 k_BT, for example, the detachment force is predicted to increase to 40 pN, whereas this ring can still move under the force of bending protofilaments. Such a ring would have no detectable diffusive motions and would therefore move exclusive by the forced-walk mechanism (Video 4). In this case, each spoke is moving along one protofilament, hopping from one binding site to another (Video 5), similar to an ATP-dependent motor enzyme, only the energy for the coupler's motion is provided by the hydrolysis of tubulin-bound GTP.

The online version of this chapter contains Video 4 and 5. The online version can be found at doi:10.1016/B978-0-08-095718-0.00409-0.

4.7.5.4   Experimental Analysis of Dam1-Dependent Coupling

Theoretical modeling has revealed the link between the strength of a ring's adhesion to the MT, the rate of that ring's diffusion, and the extent to which a ring with no load should slow the rate of MT depolymerization.[69] All these and other Dam1-dependent phenomena reflect aspects of the interactions between Dam1 heterodecamers and the MT wall, so their quantitative characteristics should correspond. However, the complexity of this system and the significant discrepancy between the published experimental measurements have

led to controversial views on the mechanism of coupling by a real Dam1 ring. Two of the most important parameters of Dam1-tubulin interaction – their binding energy and the rate of Dam1 diffusion on the MT surface – are still being debated.

Westermann et al.[90] used a biochemical approach to estimate the dissociation constant between the Dam1 heterodecamer and MTs; their data suggested that this value is in the submicromolar range. Without knowledge of the pathway for Dam1 oligomerization and MT binding, however, this constant does not define the tubulin-Dam1 binding energy unambiguously. Some of the observed binding energy may have been the result of Dam1-Dam1 interactions, so this value can be used only as an upper estimate for Dam1-MT binding (≈ 15 k_BT). However, the MT affinity of a mutant Dam1 complex with reduced ability to form rings is similar to that of wild-type Dam1,[50,90] suggesting that a large fraction of the observed interaction corresponds to Dam1-MT binding. More recently, Gestaut et al.[36] concluded, using a microscopy-based assay, that Dam1-MT affinity is two orders of magnitude stronger. One can show, however, that GTP hydrolysis cannot provide enough energy to move a ring with binding this strong.

The most straightforward measure of the interaction between a Dam1 ring and the MT it surrounds comes from an *in vitro* analysis of the rate of ring motion with no load (**Figure 6(c)**).[43] The observed rate with which a Dam1 ring tracks the shortening MT implies an energy of 13 to 15 k_BT per Dam1-tubulin bond, consistent with biochemical data.[90] As stated earlier, a ring with such moderately strong bonds should not show observable diffusion on a biologically relevant timescale of many minutes. The first published report of this kind, however, concluded that the Dam1 rings diffused very quickly (0.05 μm^2 s^{-1}),[44] although this interpretation did not take into account the ability of Dam1 heterodecamers to form various oligomeric complexes which differ in size and geometric configuration.[42] Subsequent quantitative studies of the diffusion of Dam1 complexes have shown that this high diffusion coefficient characterized the thermal motions of only one to two Dam1 subunits[36,42]; larger Dam1 oligomers diffuse much more slowly.[42] These observations estimate the diffusion of a full Dam1 ring at 10^{-7} μm^2 s^{-1}, suggesting more than 7 k_BT energy of Dam1-tubulin binding.

For a detailed review of other experimental observations and their theoretical analysis the authors refer readers to their previous publication.[43] Based on the previously cited data and the authors' other observations with fluorescently labeled, wild-type, and mutant Dam1 complexes, and based on the analysis of motions of Dam1-coated beads and measurement of the associated forces, the authors conclude that a Dam1 ring behaves very much as predicted by a model of the forced-walk mechanism. The biomechanical properties of the Dam1 ring (its large diameter, flexible spokes, and relatively strong binding) are finely tuned to enable this coupler to move under load without detaching. Video 6, that is based on the mathematical model of a depolymerizing MT, depicts a strongly binding ring and an attached 0.5-μm bead; it illustrates many of these features. When the tracking ring stalls in this sequence, the flared protofilaments continue their shortening, and the splitting between adjacent protofilaments propagates

into the MT wall downstream from the ring. The MT begins to lose its integrity, but the strongly attached ring impedes further protofilament splaying, and the ring maintains its association with the shortening MT end. When the opportunity subsequently arises, the ring moves swiftly forward, and the bead continues its motion. A coupler like this would be particularly useful in budding yeast, in which each kinetochore is stably attached to only one MT,[86] such that the coupler must maintains its attachment, even under an opposing force and despite the significant stochasticity of tubulin dynamics.

The online version of this chapter contains Video 6. The online version can be found at doi:10.1016/B978-0-08-095718-0.00409-0.

Although this view is very appealing, further work is required to understand more completely the biophysical mechanism of Dam1 ring motility. In addition to determining the Dam1-MT binding affinity and diffusion properties of different Dam1 oligomers, future experiments should also address the force generation by an MT encircled by a Dam1 ring. Two current measurements show less than 5 pN force,[43,75] which is interpreted very differently by these studies (with or without considering the attenuating 'lever-arm' effect described in Section 4.7.4.3), so this issue also remains controversial.

4.7.5.5   On the Mechanism of Motion of Protein-Coated Beads with MT Disassembly

Research aimed at understanding the mechanisms which ensure stable chromosomal attachment to shortening MT ends has received a boost during the past decade, thanks to the identification and purification of many kinetochore-associated protein complexes (reviewed in Refs. 93 and 94). Several of these proteins have been conjugated to microbeads and examined for their ability to follow MT depolymerization. This has become one of the most informative *in vitro* approaches to the study of MT depolymerization-dependent forces and the coupling properties of these proteins.[70,77] Original experiments demonstrating that MT depolymerization alone can support the motion of protein-coated beads *in vitro* were carried out with MT-dependent motors in the absence of ATP.[30] A chimeric *Drosophila* kinesin NK350, that combined the motor domain of kinesin heavy chain with the stalk of NCD kinesin,[95] lacked a traditional ATP-dependent motility but was particularly successful in coupling beads to MT depolymerization. Strikingly, the NK350-coated beads moved significantly faster than the normal rate of MT depolymerization, so they appeared to induce MT disassembly. When attached to the coverslip in a traditional MT-gliding assay, NK350 chimera supported diffusive motions of stable MTs.[30] This correlative link between a protein's diffusive behavior and its ability to support bead coupling has promoted two hypotheses to explain bead motions: (1) that NK350 carried the bead toward the minus-MT end by stepping in this direction under the pushing force of bending protofilaments[30] and (2) that beads moved with the shortening MT ends via rotational diffusion.[96,97]

Recently, Westermann et al. and then the Asbury lab have reported MT depolymerization-dependent motions of

microbeads coated with Dam1 complexes.[44,75] Because structural data had provided compelling evidence that Dam1 can oligomerize into rings around stabilized MTs *in vitro*, it was assumed that the Dam1-coated beads were carried exclusively by MT-encircling rings. This view has subsequently been challenged by the analysis of a large number of Dam1-coated beads under well-controlled experimental conditions, that revealed that Dam1-coated beads can move by two distinct mechanisms.[42] These beads can bind to MTs with the help of ringlike structures only if soluble Dam1 is present in addition to the Dam1 protein which is conjugated to the bead's surface. The three most convincing biophysical arguments that support the ring coupling come from (1) a comparison of the forces transmitted under these conditions with those obtained in experiments with laterally attached beads (**Figure 6(d)**); (2) the observation that in the presence of soluble Dam1, beads are carried by the shortening MTs without detectable bead rotation, an expected configuration if the bead is coupled via a ringlike structure (Video 7); and (3) that in the presence of soluble Dam1, beads move in association with MT shortening at rates similar to those seen for ring-size Dam1 complexes with no beads.

The online version of this chapter contains Video 7. The online version can be found at doi:10.1016/B978-0-08-095718-0.00409-0.

An additional feature of Dam1-coated bead motion in the absence of soluble Dam1 is that this 'load' accelerates the rate of MT depolymerization, causing the MT to depolymerize and the bead to move much faster than in the presence of Dam1 complexes alone. The similarity between this motion and that of the NK350-coated beads, that were almost certainly not coupled by ringlike structures, prompted a direct test of the idea that such fast motions could result from bead rolling. In the absence of soluble Dam1, the Dam1-coated beads had significantly higher rotational mobility than in its presence,[42] and some beads were observed to make one or more full rotations while moving with the shortening MT (Video 8). This type of motion is probably fundamentally different from the coupling mechanisms used by mitotic chromosomes, that obviously do not roll. The specific properties of protein couplers, such as Dam1 and perhaps NK350, which enable such motility are not yet known, but they are likely to involve at least two properties: a moderately strong MT binding and a flexibility in the protein domain which links the spherical surface with the MT binding site.

The online version of this chapter contains Video 8. The online version can be found at doi:10.1016/B978-0-08-095718-0.00409-0.

4.7.5.6   Fibrillar Complexes, Rather than Rings, May Serve as Processive Couplers in Mammalian Cells

Experiments with protein-conjugated beads have revealed that numerous protein complexes can support some MT depolymerization-dependent bead motility. So far, Dam1 remains the best studied. Only one other protein – the fission yeast heterodimeric kinesin-like protein Klp5/6, has been shown to support the biologically interesting, rotation-free bead motion.[98] The ability of other couplers to move beads with no

rotation has not yet been established. These other, potentially interesting couplers include two kinetochore complexes containing the Ska1 protein, which may be a Dam1 counterpart in higher eukaryotic cells.[99] The full Ska1 complex moves the beads detectably slower than the smaller, two-subunit complex, indicating that these two motions may be driven by different mechanisms. The inhibition of MT depolymerization by full Ska1 complexes suggests that these oligomers provide cross-bridging of adjacent MT protofilaments, analogous to that provided by Dam1-containing rings.

Much current work is focused on the multisubunit Ndc80 complex, which is found at the kinetochores of all eukaryotes so far examined.[37,87] This is a highly elongated protein complex (about 60 nm),[93] which provides an essential MT binding activity for the kinetochore and is likely to contribute to its characteristic meshlike structure as seen by electron tomography (Video 9). These and structurally similar proteins are particularly interesting candidates for kinetochore couplers, because electron tomography of mammalian kinetochores has found some slender fibrils connecting curved protofilaments directly to the inner kinetochore (**Figure 6(e)**). A quantitative study of the shape of kinetochore-associated MT ends has found that the protofilaments of these MTs are differently shaped from the protofilaments at the ends of MTs growing or shortening *in vitro*.[87] The fibril-protofilament associations correlate with a local straightening of the flared kinetochore protofilaments, suggesting that these conformational changes are brought about by forces acting through the fibrils.

The online version of this chapter contains Video 9. The online version can be found at doi:10.1016/B978-0-08-095718-0.00409-0.

These experimental findings have inspired ideas about a possible ring-independent mechanism for harnessing MT dynamics directly to cargo movement.[87] A corresponding mathematical model is based on the previously described molecular-mechanical model for depolymerizing MTs, modified to include extended elements (kinetochore fibrils) which connect the tubulin in flaring protofilaments with cargo. The fibrils were assumed to be present in nonlimiting quantities and to be able to bind at random places along the protofilaments, although not to soluble tubulin. As protofilaments tended toward their minimum energy conformation, they exerted a power stroke on the associated fibril, thereby leading to the cargo's motion. When tubulin depolymerized from the tip of a bending protofilament, any associated fibril was released, and could then join the pool of fibrils which interacted randomly with binding sites on the MT. With these assumptions, the model demonstrated that protofilament power strokes could move a cargo steadily against a significant load (Video 10). In fact, fibrillar coupling is predicted to be more energy efficient than the Dam1 ring (**Figure 6(f)**). A ring which binds MTs strongly enough to provide processive coupling impedes MT shortening and reduces the useful work which MT depolymerization can accomplish.[43] In contrast, the fibril-based coupler is not forced to walk from one binding site to the next on the MT wall; the fibrils undergo cycles of detachment and reattachment, so the efficiency of the depolymerization motor is not limited. This feature might be particularly valuable in cells where chromosomes are large and/or experience significant opposing force to

their motion. However, the fibrils have a clear disadvantage; they connect to the MT protofilaments stochastically and independently of one another. Thus, if some of them failed to form lasting connections, the unbound protofilaments could peel away from their load (Video 11). In the model, the cargo's motion is then stalled. In a real MT such a configuration is likely to disintegrate, so the load would probably become lost. Thus, this type of coupling may only work in cells in which the kinetochores are attached to numerous MTs; a loss of one such connection would not have serious consequences.

The online version of this chapter contains Video **10** and **11**. The online version can be found at doi:10.1016/B978-0-08-095718-0.00409-0.

This fibril-based model is far from providing satisfactory answers to all physiological questions about MT-kinetochore coupling. For example, it does not explain how chromosomes can move at the ends of elongating MTs. Rather, this model should be viewed as a prototype of a novel coupling strategy which is driven by the power stroke-dependent mechanism and does not rely on a rigid, encircling structure, but can work without any sliding along the MT wall. An alternative view of coupling by fibrils is based on a biased-diffusion mechanism.[37] This model has been described to involve multiple MT-binding fibrils (e.g., Ndc80 complexes). The associated calculations were, however, carried out with equations which Hill wrote for his sleeve, where all binding proteins moved in synchrony and were prevented from dissociation from the MT wall by the rigid structure of the sleeve. In the fibrillar biased-diffusion model,[37] the MT-binding fibrils have no length and no characteristics to describe their physical properties. It therefore appears that a rigorous comparison of power stroke-dependent and biased diffusion-based fibrous couplers has not yet been accomplished, because the postulates of the Hill sleeve are not all applicable to the less-ordered, fibril-based coupling. Although Ndc80-coated beads have been shown to follow the shortening MT ends[87] in the presence of as much as a 2.5-pN load,[37] it is not yet known whether these beads move by any of these two mechanism, and their possible rolling has not been ruled out.

4.7.6   Summary

MTs are components of the eukaryotic cytoskeleton important for cell structure and function. Growing MTs can generate pushing forces, which contribute to motions of cellular organelles, and to normal cell shape and polarity. MTs are essential for chromosome motion during cell division, in part because they serve as tracks for the motion of mitotic motor enzymes, and in part because of the ability of depolymerizing MTs to generate pulling forces. These forces can be thermal in origin, working by a biased-diffusing mechanism, or they can arise from the unique mechanochemical features of tubulin polymerization. Each MT is like a loaded spring because tubulin-associated GTP is hydrolyzed during tubulin polymerization. Some of the energy so liberated is stored in conformational strain in the MT wall and is released by the bending of tubulin during its depolymerization. Linear strands of tubulin, called 'protofilaments', curve as they depolymerize, which lets them

work as motors. Theory predicts that the resulting force can be large, which helps to explain experimental observations that motions of mitotic chromosomes can be driven by MT depolymerization alone. Modeling of depolymerization-dependent motility emphasizes the significant differences in the mechanisms of the motions of laterally attached microbeads which are driven by MT depolymerization vs. traditional ATP-dependent motors. Recent years have seen significant progress in the experimental analysis of the power strokes available from bending protofilaments; the experimental data fit well with model predictions, but the direct measure of large depolymerization forces is still lacking.

In cells, kinetochore-MT connections are maintained even in the presence of large opposing forces and despite the stochasticity of tubulin dynamics. These functions are thought to be carried out by kinetochore-localized couplers, the macromolecular complexes which capture the energy from MT disassembly and provide lasting attachments to shortening MT ends. Several couplers – one based on a sleeve, one on a ring, and a third on elongated fibrils – have now been studied theoretically, so one can compare their characteristic features, such as their efficiencies of energy transduction, stabilities of attachment, and force-velocity relationships. Ring-based coupling is particularly well understood; discovery of the multiprotein Dam1 ring has allowed an in-depth analysis of its design and function. The biomechanical properties of the yeast Dam1 ring, such as its large diameter, flexible spokes, and relatively strong binding, appear to be finely tuned to enable this coupler to move under load without detaching. Current work is focused on quantitative analyses of other multiprotein kinetochore complexes which are likely candidates for fibril-based processive couplers in mammalian cells.

References

[1] Mogilner, A. On the edge: modeling protrusion. *Curr. Opin. Cell Biol.* **2006**, *18*, 32–39.

[2] Footer, M. J.; Kerssemakers, J. W.; Theriot, J. A.; Dogterom, M. Direct measurement of force generation by actin filament polymerization using an optical trap. *Proc. Natl. Acad. Sci. USA* **2007**, *104*, 2181–2186.

[3] Gerdes, K.; Moller-Jensen, J.; Ebersbach, G.; Kruse, T.; Nordstrom, K. Bacterial mitotic machineries. *Cell* **2004**, *116*, 359–366.

[4] Tilney, L. G.; Porter, K. R. Studies on the microtubules in heliozoa. II. The effect of low temperature on these structures in the formation and maintenance of the axopodia. *J. Cell Biol.* **1967**, *34*, 327–343.

[5] Tran, P. T.; Marsh, L.; Doye, V.; Inoue, S.; Chang, F. A mechanism for nuclear positioning in fission yeast based on microtubule pushing. *J. Cell Biol.* **2001**, *153*, 397–411.

[6] Yaffe, M. P.; Stuurman, N.; Vale, R. D. Mitochondrial positioning in fission yeast is driven by association with dynamic microtubules and mitotic spindle poles. *Proc. Natl. Acad. Sci. USA* **2003**, *100*, 11424–11428.

[7] Waterman-Storer, C. M.; Salmon, E. D. Endoplasmic reticulum membrane tubules are distributed by microtubules in living cells using three distinct mechanisms. *Curr. Biol.* **1998**, *8*, 798–806.

[8] Dogterom, M.; Yurke, B. Measurement of the force-velocity relation for growing microtubules. *Science* **1997**, *278*, 856–860.

[9] Miyamoto, H.; Hotani, H. Polymerization of microtubules in liposomes produces morphological changes of shape. *Proc. Tanaguichi Int. Symp.* **1988**, *14*, 220–242.

[10] Fygenson, D. K.; Marko, J. F.; Libchaber, A. Mechanics of microtubule-based membrane extension. *Phys. Rev. Lett.* **1997**, *79*, 4497–4500.

[11] Dogterom, M.; Janson, M. E.; Faivre-Moskalenko, C.; van der Horst, A.; Kerssemakers, J. W. J.; Tanase, C.; Mulder, B. M. Force generation by polymerizing microtubules. *Appl. Phys. A* **2002**, *75*, 331–336.

[12] Dogterom, M.; Kerssemakers, J. W.; Romet-Lemonne, G.; Janson, M. E. Force generation by dynamic microtubules. *Curr. Opin. Cell Biol.* **2005**, *17*, 67–74.

[13] Hamaguchi, S.; Hiramoto, Y. Analysis of the role of astral rays in pronuclear migration in sand dollar eggs by the Colcemid-UV method. *Dev. Growth Diff.* **1985**, *28*, 143–156.

[14] Tischer, C.; Brunner, D.; Dogterom, M. Force- and kinesin-8-dependent effects in the spatial regulation of fission yeast microtubule dynamics. *Mol. Syst. Biol.* **2009**, *5*, 250.

[15] Foethke, D.; Makushok, T.; Brunner, D.; Nedelec, F. Force- and length-dependent catastrophe activities explain interphase microtubule organization in fission yeast. *Mol. Syst. Biol.* **2009**, *5*, 241.

[16] Peskin, C. S.; Odell, G. M.; Oster, G. F. Cellular motions and thermal fluctuations: the Brownian ratchet. *Biophys. J.* **1993**, *65*, 316–324.

[17] Kolomeisky, A. B.; Fisher, M. E. Force-velocity relation for growing microtubules. *Biophys. J.* **2001**, *80*, 149–154.

[18] Mogilner, A.; Oster, G. Cell motility driven by actin polymerization. *Biophys. J.* **1996**, *71*, 3030–3045.

[19] Gittes, F.; Meyhofer, E.; Baek, S.; Howard, J. Directional loading of the kinesin motor molecule as it buckles a microtubule. *Biophys. J.* **1996**, *70*, 418–429.

[20] Mogilner, A.; Oster, G. The polymerization ratchet model explains the force-velocity relation for growing microtubules. *Eur. Biophys. J. Biophys. Lett.* **1999**, *28*, 235–242.

[21] Janson, M. E.; de Dood, M. E.; Dogterom, M. Dynamic instability of microtubules is regulated by force. *J. Cell Biol.* **2003**, *161*, 1029–1034.

[22] Kerssemakers, J. W.; Munteanu, E. L.; Laan, L.; Noetzel, T. L.; Janson, M. E.; Dogterom, M. Assembly dynamics of microtubules at molecular resolution. *Nature* **2006**, *442*, 709–712.

[23] Janson, M. E.; Dogterom, M. Scaling of microtubule force-velocity curves obtained at different tubulin concentrations. *Phys. Rev. Lett.* **2004**, *92*, 248101.

[24] van Doorn, G. S.; Tanase, C.; Mulder, B. M.; Dogterom, M. On the stall force for growing microtubules. *Eur. Biophys. J.* **2000**, *29*, 2–6.

[25] Schek, III H. T.; Gardner, M. K.; Cheng, J.; Odde, D. J.; Hunt, A. J. Microtubule assembly dynamics at the nanoscale. *Curr. Biol.* **2007**, *17*, 1445–1455.

[26] Molodtsov, M. I.; Ermakova, E. A.; Shnol, E. E.; Grishchuk, E. L.; McIntosh, J. R.; Ataullakhanov, F. I. A molecular-mechanical model of the microtubule. *Biophys. J.* **2005**, *88*, 3167–3179.

[27] Molodtsov, M. I.; Grishchuk, E. L.; Efremov, A. K.; McIntosh, J. R.; Ataullakhanov, F. I. Force production by depolymerizing microtubules: a theoretical study. *Proc. Natl. Acad. Sci. USA* **2005**, *102*, 4353–4358.

[28] VanBuren, V.; Cassimeris, L.; Odde, D. J. Mechanochemical model of microtubule structure and self-assembly kinetics. *Biophys. J.* **2005**, *89*, 2911–2926.

[29] Coue, M.; Lombillo, V. A.; McIntosh, J. R. Microtubule depolymerization promotes particle and chromosome movement. *in vitro. J. Cell Biol.* **1991**, *112*, 1165–1175.

[30] Lombillo, V. A.; Stewart, R. J.; McIntosh, J. R. Minus-end-directed motion of kinesin-coated microspheres driven by microtubule depolymerization. *Nature* **1995**, *373*, 161–164.

[31] Grishchuk, E. L.; McIntosh, J. R. Microtubule depolymerization can drive poleward chromosome motion in fission yeast. *EMBO J.* **2006**, *25*, 4888–4896.

[32] Tanaka, K.; Kitamura, E.; Kitamura, Y.; Tanaka, T. U. Molecular mechanisms of microtubule-dependent kinetochore transport toward spindle poles. *J. Cell Biol.* **2007**, *178*, 269–281.

[33] Ringgaard, S.; van, Z. J.; Howard, M.; Gerdes, K. Movement and equipositioning of plasmids by ParA filament disassembly. *Proc. Natl. Acad. Sci. USA* **2009**, *106*, 19369–19374.

[34] Fox, R. F. Rectified Brownian movement in molecular and cell biology. *Phys. Rev. E* **1997**, *57*, 2177–2203.

[35] Mai, J.; Sokolov, I. M.; Blumen, A. Directed particle diffusion under "burnt bridges" conditions. *Phys. Rev. E Stat. Nonlin. Soft. Matter Phys.* **2001**, *64*, 011102.

[36] Gestaut, D. R.; Graczyk, B.; Cooper, J.; Widlund, P. O.; Zelter, A.; Wordeman, L.; Asbury, C. L.; Davis, T. N. Phosphoregulation and depolymerization-driven movement of the Dam1 complex do not require ring formation. *Nat. Cell Biol.* **2008**, *10*, 407–414.

[37] Powers, A. F.; Franck, A. D.; Gestaut, D. R.; Cooper, J.; Gracyzk, B.; Wei, R. R.; Wordeman, L.; Davis, T. N.; Asbury, C. L. The Ndc80 kinetochore complex forms load-bearing attachments to dynamic microtubule tips via biased diffusion. *Cell* **2009**, *136*, 865–875.

[38] Ali, M. Y.; Krementsova, E. B.; Kennedy, G. G.; Mahaffy, R.; Pollard, T. D.; Trybus, K. M.; Warshaw, D. M. Myosin Va maneuvers through actin intersections and diffuses along microtubules. *Proc. Natl. Acad. Sci. USA* **2007**, *104*, 4332–4336.

[39] Ermak, D. L.; McCammon, J. A. Brownian dynamics with hydrodynamic interactions. *J. Chem. Phys.* **1978**, *69*, 1352–1360.

[40] Salmon, E. D.; Saxton, W. M.; Leslie, R. J.; Karow, M. L.; McIntosh, J. R. Diffusion coefficient of fluorescein-labeled tubulin in the cytoplasm of embryonic cells of a sea urchin: video image analysis of fluorescence redistribution after photobleaching. *J. Cell Biol.* **1984**, *99*, 2157–2164.

[41] Cooper, J. R.; Wordeman, L. The diffusive interaction of microtubule binding proteins. *Curr. Opin. Cell Biol.* **2009**, *21*, 68–73.

[42] Grishchuk, E. L.; Spiridonov, I. S.; Volkov, V. A.; Efremov, A.; Westermann, S.; Drubin, D.; Barnes, G.; Ataullakhanov, F. I.; McIntosh, J. R. Different assemblies of the DAM1 complex follow shortening microtubules by distinct mechanisms. *Proc. Natl. Acad. Sci. USA* **2008**, *105*, 6918–6923.

[43] Grishchuk, E. L.; Efremov, A. K.; Volkov, V. A.; Spiridonov, I. S.; Gudimchuk, N.; Westermann, S.; Drubin, D.; Barnes, G.; McIntosh, J. R.; Ataullakhanov, F. I. The Dam1 ring binds microtubules strongly enough to be a processive as well as energy-efficient coupler for chromosome motion. *Proc. Natl. Acad. Sci. USA* **2008**, *105*, 15423–15428.

[44] Westermann, S.; Wang, H. W.; Avila-Sakar, A.; Drubin, D. G.; Nogales, E.; Barnes, G. The Dam1 kinetochore ring complex moves processively on depolymerizing microtubule ends. *Nature* **2006**, *440*, 565–569.

[45] Hill, T. L. Theoretical problems related to the attachment of microtubules to kinetochores. *Proc. Natl. Acad. Sci. USA* **1985**, *82*, 4404–4408.

[46] Joglekar, A. P.; Hunt, A. J. A simple, mechanistic model for directional instability during mitotic chromosome movements. *Biophys. J.* **2002**, *83*, 42–58.

[47] Nicklas, R. B. Measurements of the force produced by the mitotic spindle in anaphase. *J. Cell Biol.* **1983**, *97*, 542–548.

[48] Jiang, L.; Gao, Y.; Mao, F.; Liu, Z.; Lai, L. Potential of mean force for protein-protein interaction studies. *Proteins* **2002**, *46*, 190–196.

[49] Drabik, P.; Gusarov, S.; Kovalenko, A. Microtubule stability studied by three-dimensional molecular theory of solvation. *Biophys. J.* **2007**, *92*, 394–403.

[50] Wang, H. W.; Ramey, V. H.; Westermann, S.; Leschziner, A. E.; Welburn, J. P.; Nakajima, Y.; Drubin, D. G.; Barnes, G.; Nogales, E. Architecture of the Dam1 kinetochore ring complex and implications for microtubule-driven assembly and force-coupling mechanisms. *Nat. Struct. Mol. Biol.* **2007**, *14*, 721–726.

[51] Gorman, J.; Greene, E. C. Visualizing one-dimensional diffusion of proteins along DNA. *Nat. Struct. Mol. Biol.* **2008**, *15*, 768–774.

[52] Zwanzig, R. Diffusion in a rough potential. *Proc. Natl. Acad. Sci. USA* **1988**, *85*, 2029–2030.

[53] Blainey, P. C.; Luo, G.; Kou, S. C.; Mangel, W. F.; Verdine, G. L.; Bagchi, B.; Xie, X. S. Nonspecifically bound proteins spin while diffusing along DNA. *Nat. Struct. Mol. Biol.* **2009**, *16*, 1224–1229.

[54] Slutsky, M.; Mirny, L. A. Kinetics of protein-DNA interaction: facilitated target location in sequence-dependent potential. *Biophys. J.* **2004**, *87*, 4021–4035.

[55] Schurr, J. M. The one-dimensional diffusion coefficient of proteins absorbed on DNA. Hydrodynamic considerations. *Biophys. Chem.* **1979**, *9*, 413–414.

[56] Tuszynski, J. A.; Brown, J. A.; Crawford, E.; Carpenter, E. J.; Nip, M. L. A.; Dixon, J. M.; Sataric, M. V. Molecular Dynamics Simulations of Tubulin Structure and Calculations of Electrostatic Properties of Microtubules. *Math. Comput. Model* **2005**, *41*, 1055–1070.

[57] Baker, N. A.; Sept, D.; Joseph, S.; Holst, M. J.; McCammon, J. A. Electrostatics of nanosystems: application to microtubules and the ribosome. *Proc. Natl. Acad. Sci. USA* **2001**, *98*, 10037–10041.

[58] Minoura, I.; Katayama, E.; Sekimoto, K.; Muto, E. One-dimensional Brownian motion of charged nanoparticles along microtubules: a model system for weak binding interactions. *Biophys. J.* **2010**, *98*, 1589–1597.

[59] Okada, Y.; Hirokawa, N. A processive single-headed motor: kinesin superfamily protein KIF1A. *Science* **1999**, *283*, 1152–1157.

[60] Bormuth, V.; Varga, V.; Howard, J.; Schaffer, E. Protein friction limits diffusive and directed movements of kinesin motors on microtubules. *Science* **2009**, *325*, 870–873.

[61] Wei, R. R.; Al-Bassam, J.; Harrison, S. C. The Ndc80/HEC1 complex is a contact point for kinetochore-microtubule attachment. *Nat. Struct. Mol. Biol.* **2007**, *14*, 54–59.

[62] Ciferri, C.; Pasqualato, S.; Screpanti, E.; Varetti, G.; Santaguida, S.; Dos, R. G.; Maiolica, A.; Polka, J.; De Luca, J. G.; De, W. P.; Salek, M.; Rappsilber, J.; Moores, C. A.; Salmon, E. D.; Musacchio, A. Implications for kinetochore-microtubule attachment from the structure of an engineered Ndc80 complex. *Cell* **2008**, *133*, 427–439.

[63] Maccioni, R.; Seeds, N. W. Stoichiometry of GTP hydrolysis and tubulin polymerization. *Proc. Natl. Acad. Sci. USA* **1977**, *74*, 462–466.

[64] Mitchison, T.; Kirschner, M. Dynamic instability of microtubule growth. *Nature* **1984**, *312*, 237–242.

[65] Nogales, E. Structural insight into microtubule function. *Annu. Rev. Biophys. Biomol. Struct.* **2001**, *30*, 397–420.

[66] Mandelkow, E. M.; Mandelkow, E.; Milligan, R. A. Microtubule dynamics and microtubule caps: a time-resolved cryo-electron microscopy study. *J. Cell Biol.* **1991**, *114*, 977–991.

[67] Koshland, D. E.; Mitchison, T. J.; Kirschner, M. W. olewards chromosome movement driven by microtubule depolymerization. *in vitro Nature* **1988**, *331*, 499–504.

[68] McIntosh, J. R.; Volkov, V.; Ataullakhanov, F. I.; Grishchuk, E. L. Tubulin depolymerization may be an ancient biological motor. *J. Cell Sci.* **2010**, *123*, 3425–3434.

[69] Efremov, A.; Grishchuk, E. L.; McIntosh, J. R.; Ataullakhanov, F. I. In search of an optimal ring to couple microtubule depolymerization to processive chromosome motions. *Proc. Natl. Acad. Sci. USA* **2007**, *104*, 19017–19022.

[70] Franck, A. D.; Powers, A. F.; Gestaut, D. R.; Davis, T. N.; Asbury, C. L. Direct physical study of kinetochore-microtubule interactions by reconstitution and interrogation with an optical force clamp. *Methods* **2010**, *51*, 242–250.

[71] Grishchuk, E. L.; Molodtsov, M. I.; Ataullakhanov, F. I.; McIntosh, J. R. Force production by disassembling microtubules. *Nature* **2005**, *438*, 384–388.

[72] Heermann, D. W. *Computer Simulation Methods in Theoretical Physics*; Springer: New York, NY, 1990.

[73] Fygenson, D. K.; Braun, E.; Libchaber, A. Phase diagram of microtubules. *Phys. Rev. E Stat. Phys. Plasmas Fluids Rel. Interdiscip. Topics* **1994**, *50*, 1579–1588.

[74] Laan, L.; Dogterom, M. *In vitro* assays to study force generation at dynamic microtubule ends. *Methods Cell Biol.* **2010**, *95*, 617–639.

[75] Asbury, C. L.; Gestaut, D. R.; Powers, A. F.; Franck, A. D.; Davis, T. N. The Dam1 kinetochore complex harnesses microtubule dynamics to produce force and movement. *Proc. Natl. Acad. Sci. USA* **2006**, *103*, 9873–9878.

[76] Tien, J. F.; Umbreit, N. T.; Gestaut, D. R.; Franck, A. D.; Cooper, J.; Wordeman, L.; Gonen, T.; Asbury, C. L.; Davis, T. N. Cooperation of the Dam1 and Ndc80 kinetochore complexes enhances microtubule coupling and is regulated by aurora B. *J. Cell Biol.* **2010**, *189*, 713–723.

[77] Grishchuk, E. L.; Ataullakhanov, F. I. *In vitro* assays to study the tracking of shortening microtubule ends and to measure associated forces. *Methods Cell Biol.* **2010**, *95*, 657–676.

[78] O'Brien, E. T.; Salmon, E. D.; Walker, R. A.; Erickson, H. P. Effects of magnesium on the dynamic instability of individual microtubules. *Biochemistry* **1990**, *29*, 6648–6656.

[79] Nicklas, R. B. How cells get the right chromosomes. *Science* **1997**, *275*, 632–637.

[80] McIntosh, J. R.; Grishchuk, E. L.; West, R. R. Chromosome-microtubule interactions during mitosis. *Annu. Rev. Cell Dev. Biol.* **2002**, *18*, 193–219.

[81] Maiato, H.; DeLuca, J.; Salmon, E. D.; Earnshaw, W. C. The dynamic kinetochore-microtubule interface. *J. Cell Sci.* **2004**, *117*, 5461–5477.

[82] Franck, A. D.; Powers, A. F.; Gestaut, D. R.; Gonen, T.; Davis, T. N.; Asbury, C. L. Tension applied through the Dam1 complex promotes microtubule elongation providing a direct mechanism for length control in mitosis. *Nat. Cell Biol.* **2007**, *9*, 832–837.

[83] Rieder, C. L.; Salmon, E. D. The vertebrate cell kinetochore and its roles during mitosis. *Trends Cell Biol.* **1998**, *8*, 310–318.

[84] Santaguida, S.; Musacchio, A. The life and miracles of kinetochores. *EMBO J.* **2009**, *28*, 2511–2531.

[85] Wollman, R.; Cytrynbaum, E. N.; Jones, J. T.; Meyer, T.; Scholey, J. M.; Mogilner, A. Efficient chromosome capture requires a bias in the 'search-and-capture' process during mitotic-spindle assembly. *Curr. Biol.* **2005**, *15*, 828–832.

[86] O'Toole, E. T.; Winey, M.; McIntosh, J. R. High-voltage electron tomography of spindle pole bodies and early mitotic spindles in the yeast. *Saccharomyces cerevisiae. Mol. Biol. Cell* **1999**, *10*, 2017–2031.

[87] McIntosh, J. R.; Grishchuk, E. L.; Morphew, M. K.; Efremov, A. K.; Zhudenkov, K.; Volkov, V. A.; Cheeseman, I. M.; Desai, A.; Mastronarde, D. N.; Ataullakhanov, F. I. Fibrils connect microtubule tips with kinetochores: a mechanism to couple tubulin dynamics to chromosome motion. *Cell* **2008**, *135*, 322–333.

[88] Shtylla, B.; Keener, J.P. A mechanomolecular model for the movement of chromosomes during mitosis driven by a minimal kinetochore bicyclic cascade. *J. Theor. Biol.* **2010**, *263*(4), 455–470.

[89] Kirschner, M. W.; Honig, L. S.; Williams, R. C. Quantitative electron microscopy of microtubule assembly. *in vitro. J. Mol. Biol.* **1975**, *99*, 263–276.

[90] Westermann, S.; Avila-Sakar, A.; Wang, H. W.; Niederstrasser, H.; Wong, J.; Drubin, D. G.; Nogales, E.; Barnes, G. Formation of a dynamic kinetochore- microtubule interface through assembly of the Dam1 ring complex. *Mol. Cell* **2005**, *17*, 277–290.

[91] Miranda, J. J.; De, W. P.; Sorger, P. K.; Harrison, S. C. The yeast DASH complex forms closed rings on microtubules. *Nat. Struct. Mol. Biol.* **2005**, *12*, 138–143.

[92] Miranda, J. J.; King, D. S.; Harrison, S. C. Protein arms in the kinetochore-microtubule interface of the yeast DASH complex. *Mol. Biol. Cell* **2007**, *18*, 2503–2510.

[93] Welburn, J. P.; Cheeseman, I. M. Toward a molecular structure of the eukaryotic kinetochore. *Dev. Cell* **2008**, *15*, 645–655.

[94] Westermann, S.; Drubin, D. G.; Barnes, G. Structures and functions of yeast kinetochore complexes. *Annu. Rev. Biochem.* **2007**, *76*, 563–591.

[95] Stewart, R. J.; Thaler, J. P.; Goldstein, L. S. Direction of microtubule movement is an intrinsic property of the motor domains of kinesin heavy chain and Drosophila ncd protein. *Proc. Natl. Acad. Sci. USA* **1993**, *90*, 5209–5213.

[96] Peskin, C. S.; Oster, G. F. Force production by depolymerizing microtubulers: load-velocity curves and run-pause statistics. *Biophys. J.* **1995**, *69*, 2268–2276.

[97] Tao, Y. C.; Peskin, C. S. Simulating the role of microtubules in depolymerization-driven transport: a Monte Carlo approach. *Biophys. J.* **1998**, *75*, 1529–1540.

[98] Grissom, P. M.; Fiedler, T.; Grishchuk, E. L.; Nicastro, D.; West, R. R.; McIntosh, J. R. Kinesin-8 from fission yeast: a heterodimeric, plus-end-directed motor that can couple microtubule depolymerization to cargo movement. *Mol. Biol. Cell* **2009**, *20*, 963–972.

[99] Welburn, J. P.; Grishchuk, E. L.; Backer, C. B.; Wilson-Kubalek, E. M.; Yates, III J. R.; Cheeseman, I. M. The human kinetochore Ska1 complex facilitates microtubule depolymerization-coupled motility. *Dev. Cell* **2009**, *16*, 374–385.